

Interplay between nuclear factor- κ B, p38 MAPK, and glucocorticoid receptor signaling synergistically induces functional TLR2 in lung epithelial cells

Received for publication, September 9, 2021, and in revised form, February 11, 2022. Published, Papers in Press, February 19, 2022.

<https://doi.org/10.1016/j.jbc.2022.101747>

Akanksha Bansal¹, Mahmoud M. Mostafa¹, Cora Kooi², Sarah K. Sasse³, Aubrey N. Michi¹, Suharsh V. Shah¹, Richard Leigh^{1,2}, Anthony N. Gerber^{3,4}, and Robert Newton^{1,*}

From the ¹Department of Physiology & Pharmacology and Airways Inflammation Research Group, Snyder Institute for Chronic Diseases, Cumming School of Medicine, and ²Department of Medicine and Airways Inflammation Research Group, Snyder Institute for Chronic Diseases, University of Calgary, Calgary, Alberta, Canada; ³Department of Medicine, National Jewish Health, Denver, Colorado, USA; ⁴Department of Medicine, University of Colorado, Aurora, Colorado, USA

Edited by Henrik Dohlman

While glucocorticoids act *via* the glucocorticoid receptor (GR; NR3C1) to reduce the expression of many inflammatory genes, repression is not an invariable outcome. Here, we explore synergy occurring between synthetic glucocorticoids (dexamethasone and budesonide) and proinflammatory cytokines (IL1B and TNF) on the expression of the toll-like receptor 2 (TLR2). This effect is observed in epithelial cell lines and both undifferentiated and differentiated primary human bronchial epithelial cells (pHBECs). In A549 cells, IL1B-plus-glucocorticoid-induced TLR2 expression required nuclear factor (NF)- κ B and GR. Likewise, in A549 cells, BEAS-2B cells, and pHBECs, chromatin immunoprecipitation identified GR- and NF- κ B/p65-binding regions \sim 32 kb (*R1*) and \sim 7.3 kb (*R2*) upstream of the *TLR2* gene. Treatment of BEAS-2B cells with TNF or/and dexamethasone followed by global run-on sequencing confirmed transcriptional activity at these regions. Furthermore, cloning *R1* or *R2* into luciferase reporters revealed transcriptional activation by budesonide or IL1B, respectively, while *R1+R2* juxtaposition enabled synergistic activation by IL1B and budesonide. In addition, small-molecule inhibitors and siRNA knockdown showed p38 α MAPK to negatively regulate both IL1B-induced TLR2 expression and *R1+R2* reporter activity. Finally, agonism of IL1B-plus-dexamethasone-induced TLR2 in A549 cells and pHBECs stimulated NF- κ B- and interferon regulatory factor-dependent reporter activity and chemokine release. We conclude that glucocorticoid-plus-cytokine-driven synergy at *TLR2* involves GR and NF- κ B acting *via* specific enhancer regions, which combined with the inhibition of p38 α MAPK promotes TLR2 expression. Subsequent inflammatory effects that occur following TLR2 agonism may be pertinent in severe neutrophilic asthma or chronic obstructive pulmonary disease, where glucocorticoid-based therapies are less efficacious.

Glucocorticoids are steroid hormones that exert their effects *via* the glucocorticoid receptor (GR; NR3C1). This

transcription factor regulates numerous physiological processes, including growth, metabolism, and immune responses. As inhaled corticosteroids, synthetic glucocorticoids are a mainstay therapy in mild-to-moderate asthma (1, 2). However, glucocorticoids exhibit reduced clinical efficacy in patients with severe neutrophilic asthma, those who smoke, or who have chronic obstructive pulmonary disease (COPD) (3). Furthermore, use of high-dose glucocorticoid therapy, with the aim of increasing clinical effectiveness, results in contraindications that include reduced hypothalamus-pituitary-adrenal axis function, weight gain, osteoporosis, and elevated blood glucose leading to diabetes (4).

In response to environmental insults and stimuli, airway epithelial cells release proinflammatory cytokines, chemokines, and inflammatory enzymes and are the major drivers of inflammation in asthma (5, 6). However, glucocorticoids, as inhaled corticosteroids, act on the airway epithelium to suppress the release of inflammatory mediators and thereby control inflammatory cell recruitment and inflammation (7, 8). Glucocorticoids bind cytoplasmic GR and promote its translocation into the nucleus. Once in the nucleus, GR homodimers bind palindromic DNA sites known as glucocorticoid response elements (GREs). These are responsible for driving glucocorticoid-induced gene expression and occur in the regulatory regions of target genes, including many metabolic genes (9–11). However, ligand-activated GR may also interact with inflammatory transcription factors, such as nuclear factor (NF)- κ B and AP-1, and this is suggested to directly promote transcriptional repression (12). Certainly, the reduced transcription of proinflammatory genes is central to the anti-inflammatory effects of glucocorticoids. Nevertheless, products of GC-induced effector genes, which include *NFKBIA* (13), *TNFAIP3* (14), *ZFP36* (15, 16), and *TSC22D3* (17–20), can downregulate the NF- κ B pathway and/or inflammatory gene expression. Similarly, the dual-specificity phosphatase (*DUSP1*) inhibits mitogen-activated protein kinase (MAPK) signaling and is strongly induced by glucocorticoids (21). Acting together, these GC-induced effectors may collectively reduce inflammatory signaling and gene expression (22, 23).

* For correspondence: Robert Newton, newton@ucalgary.ca.

Cytokine and glucocorticoid synergy on TLR2 expression

However, colocalization of GR- and NF- κ B-binding sites in gene regulatory regions can produce GR/NF- κ B cooperation leading to enhanced transcription (24). Such effects have been reported for multiple genomic loci, with specific examples of positive GR/NF- κ B cooperativity occurring at the *TNFAIP3* and *IRAK3* genes (25–27). Such GR/NF- κ B interactions ensure that inflammation-induced feedback control of NF- κ B by TNFAIP3 is maintained, or even enhanced, in the presence of glucocorticoid (14). Comparable, and also beneficial, interactions produce transcriptional synergy between inflammatory stimuli and glucocorticoids on *IRAK3* expression (27). This is a dominant negative IL1 receptor-associated kinase that reduces signaling from IL1 receptors. Conversely, reductions in MAPK activity due to GC-induced DUSP1 appear to enhance expression of the proinflammatory transcription factor, interferon regulatory factor (IRF), IRF1 (28). Thus, glucocorticoid-activated mechanisms may increase the expression of inflammatory genes, whether these gene are proinflammatory or anti-inflammatory in effect (23).

Another gene that is believed to be NF- κ B-dependent and also is induced by glucocorticoids is the toll-like receptor (TLR), *TLR2* (17, 29–31). Toll-like receptors are pattern-recognition receptors that play pivotal roles in the cellular sensing of pathogens. Ultimately, TLR activation results in transcriptional control of various host defense molecules, including cytokines, chemokines, and other inflammatory genes (32). For example, TLR2 mediates inflammatory responses following agonism by multiple molecular patterns, including gram-positive bacterial cell wall components, such as peptidoglycan, lipoprotein, and lipoteichoic acids (33–35). Furthermore, while overexpression of DUSP1 can upregulate cytokine-induced TLR2 expression (28, 31), the mechanisms behind these effects have not been extensively studied. In the current study, transcriptional interaction between NF- κ B and GR, which both bind to the *TLR2* promoter, combined with inhibition of p38 α MAPK, are shown to induce TLR2 expression. This contributes to the synergy between

glucocorticoids and inflammatory cytokines on TLR2 expression and the effect occurs in cell lines and primary human bronchial epithelial cells (pHBECs). Agonism of interleukin-1 β (IL1B)-plus-dexamethasone-induced TLR2 induced NF- κ B and IRF1 reporter activity and promoted release of proinflammatory chemokines. Thus, glucocorticoids and NF- κ B interact positively to elicit proinflammatory effects downstream of TLR2. These findings are likely to have clinical implications in inflammatory diseases, including severe asthma where glucocorticoids show reduced clinical utility.

Results

Upregulation of TLR2 protein by proinflammatory cytokines and glucocorticoids

IL1B, at 1 ng/ml, and tumor necrosis factor α (TNF), at 10 ng/ml, produce maximal, or near maximal, NF- κ B DNA-binding and reporter activity as well as cytokine release (36–38). In A549 cells, these concentrations of IL1B and TNF, each modestly induced TLR2 protein at 6 h, with greater increases at 24 h (Figs. 1A and S1B). Similarly, the conventional glucocorticoids, dexamethasone, and budesonide, which induce near identical gene expression profiles in A549 cells (20), produce maximal activation of GRE-dependent transcription and expression of glucocorticoid-induced genes at 1 μ M and 300 nM, respectively (18, 39, 40). While dexamethasone, at 1 μ M, showed little effect on TLR2 expression, cotreatment with IL1B (Fig. 1A) or TNF (Fig. S1B) markedly enhanced TLR2 expression at both 6 and 24 h. Greatest TLR2 expression occurred at 24 h and this was confirmed by time course analysis with IL1B-plus-dexamethasone (Fig. S1A). These data suggest *supra*-additivity, a phenomenon which is defined as where the two treatments combine in a manner that is more than simply additive. Indeed, comparing the addition (*sum*) of the effects produced by IL1B and dexamethasone alone (*i.e.*, fold IL1B-1 + fold dexamethasone-1) with the effect of cotreatment (fold IL1B+dexamethasone-1) (*comb*) showed

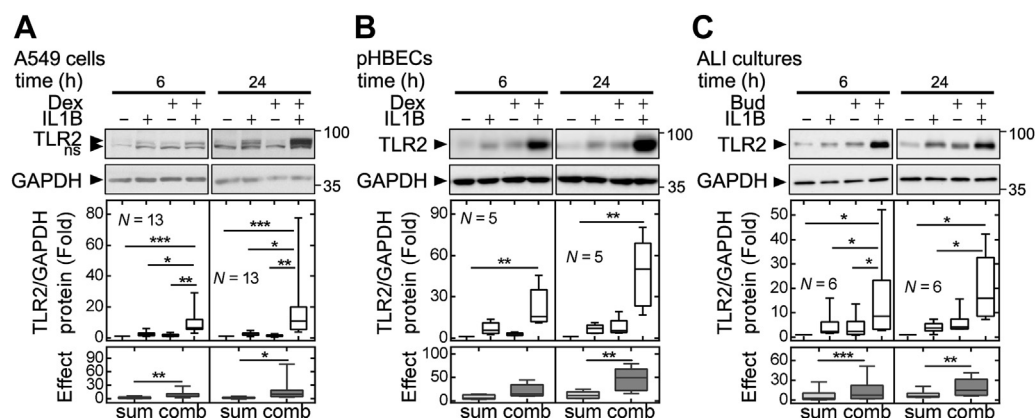


Figure 1. Combinatorial effect of IL1B and glucocorticoid on TLR2 protein expression. A, A549 cells, or pHBECs grown in B, submersion culture, or C, at air-liquid interface (ALI) were either not treated or treated with IL1B (1 ng/ml) and/or dexamethasone (Dex; 1 μ M) or budesonide (Bud; 300 nM), as indicated. The cells were harvested at 6 or 24 h for western blot analysis of TLR2 and GAPDH. Representative blots are shown. ns = non-specific band. Upper graphs, densitometric data from *N* independent experiments, normalized to GAPDH, were expressed as fold of untreated. Significance was tested using ANOVA with a Sidak post-hoc test. Lower panels, the sum effect (*i.e.*, fold - 1) for each treatment (*sum*) and the effect (fold - 1) for the combination treatment (*comb*) is plotted. The significance was tested using paired *t* test. **p* \leq 0.05, ***p* \leq 0.01, ****p* \leq 0.001. pHBEC, primary human bronchial epithelial cell; TLR, toll-like receptor.

Cytokine and glucocorticoid synergy on TLR2 expression

that the combination effect on TLR2 expression was significantly more than the sum of the effects (Fig. 1A, lower panel). This confirms *supra*-additivity in respect of TLR2 expression induced by IL1B-plus-dexamethasone and similar effects occurred with TNF-plus-dexamethasone (Fig. S1B, lower panel). In bronchial epithelial BEAS-2B cells, TNF increased TLR2 protein by 4.0-fold at 6 h, with further increases to ~15-fold at 24 h (Fig. S1C). Dexamethasone alone had no obvious effect at either time. TNF-plus-dexamethasone treatment significantly increased TLR2 protein to 6.2-fold at 6 h, and the effect of the combination was significantly greater than the sum of the effects of each treatment (Fig. S1C, lower panel). This supports *supra*-additivity at 6 h. However, at 24 h, TLR2 expression was further increased by TNF, but modestly reduced by dexamethasone.

Using pHBECS grown in submersion culture, TLR2 protein revealed greater fold increases in response to IL1B and dexamethasone when compared to A549 cells (Fig. 1B). IL1B combined with dexamethasone markedly increased TLR2 expression at 6 and 24 h, such that TLR2 expression induced by IL1B-plus-dexamethasone was significantly greater than by

each treatment alone (Table S1A). This was maximal at 24 h and the effect of IL1B-plus-dexamethasone was significantly more than the sum of the effects produced by IL1B and dexamethasone alone (Fig. 1B, lower panel). Similar outcomes and *supra*-additivity occurred in pHBECS grown as air-liquid interface (ALI) cultures using IL1B and budesonide as stimuli (Fig. 1C and Table S1B). Therefore, in each of the above cases, more than simple additivity between proinflammatory cytokines and glucocorticoids on TLR2 protein expression was revealed in epithelial cell lines and primary human airway epithelial cells.

Synergistic induction of TLR2 mRNA by proinflammatory cytokines and glucocorticoids

In A549 cells, IL1B produced a modest (<5-fold) increase in TLR2 mRNA that was maximal from 4 to 6 h (Fig. 2A). While dexamethasone alone was largely without effect, IL1B-plus-dexamethasone markedly enhanced TLR2 mRNA expression. This peaked 6 h post-stimulation, before declining steeply by 8 h with a more gradual reduction by

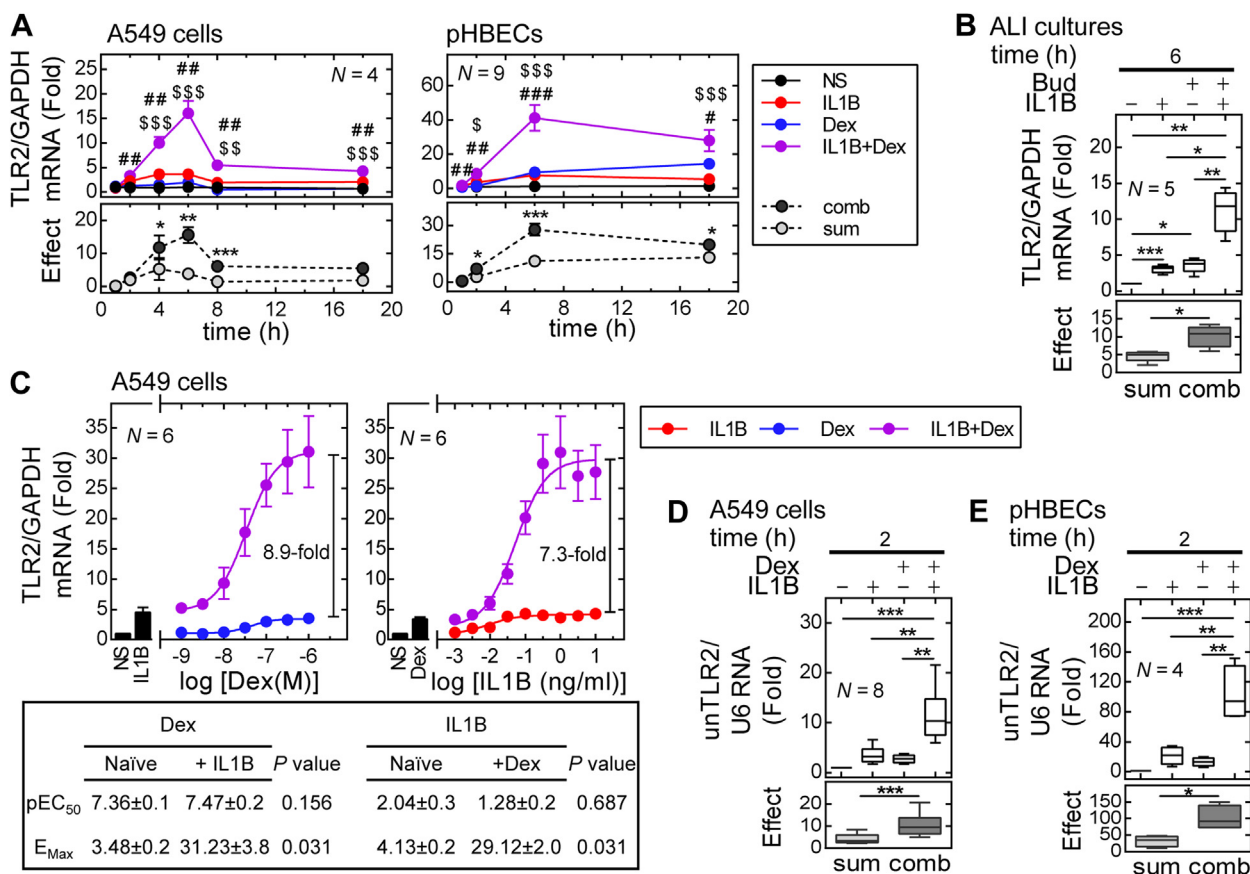


Figure 2. Proinflammatory cytokines and glucocorticoids synergistically induce TLR2 mRNA and transcription. A, A549 cells, or pHBECS grown in submersion culture, or B, pHBECS cultured at air-liquid interface (ALI) were either not stimulated (NS) or treated with IL1B (1 ng/ml) and/or dexamethasone (Dex; 1 μ M) or budesonide (Bud; 300 nM) for the times indicated. C, A549 cells were treated with IL1B and Dex, as indicated, for 6 h. A–C, cells were harvested for qPCR analysis. TLR2 data from *N* independent experiments were normalized to GAPDH and plotted as fold of NS (of the earliest time point/graph). D, A549 cells and E, pHBECS grown in submersion culture were treated as in A and harvested after 2 h for qPCR analysis of unTLR2 and U6. Data (upper panels) from *N* independent experiments were normalized to U6 and are plotted as fold relative to untreated control. Significance was tested using ANOVA with a Sidak post-hoc test. In A, ‘\$’ and ‘#’ represent significance relative to IL1B and Dex, respectively. In A, B, D, and E (lower panels), the sum effect (i.e., fold - 1) of both treatments (sum) and the effect (fold - 1) for the combination treatment (comb) is plotted. Significance at each time was tested by paired *t* test. **p* < 0.05, ***p* < 0.01, ****p* < 0.001. pHBEC, primary human bronchial epithelial cell; qPCR, quantitative PCR; TLR, toll-like receptor; unRNA, unspliced nuclear RNA.

Cytokine and glucocorticoid synergy on TLR2 expression

18 h. Comparing the sum of the effects of IL1B and dexamethasone alone with the combined effect of IL1B-plus-dexamethasone indicated *supra*-additivity at 4, 6, and 8 h (Fig. 2A, lower panel). TNF-treated A549 cells also demonstrated significantly increased TLR2 mRNA at 6 and 24 h (Fig. S2A). Dexamethasone alone was without effect but enhanced TNF-induced TLR2 mRNA expression at 6 and 24 h. This was significantly greater than the sum of individual effects of TNF and dexamethasone at 6 h and, with a similar trend at 24 h, shows *supra*-additivity (Fig. S2A, lower panel). Similar combinatorial effects were also evident for IL1B-plus-budesonide (Fig. S2B). In BEAS-2B cells, dexamethasone alone had no effect and TNF induced TLR2 mRNA at both 6 and 24 h (Fig. S2C). Comparing the sum of the effects of TNF and dexamethasone with the combination effect indicated *supra*-additivity at 6 h, but not at 24 h (Fig. S2C, lower panel). Likewise, pHBECs grown in submersion culture showed increased TLR2 mRNA expression following treatment with IL1B, TNF, or dexamethasone (Figs. 2A and S2D). Toll-like receptor 2 mRNA expression was further increased by IL1B-, or TNF-, plus-dexamethasone cotreatment with *supra*-additivity apparent from 2 h onward for IL1B-plus-dexamethasone or from 6 h with TNF-plus-dexamethasone (Figs. 2A and S2D). In ALI culture of pHBECs, both IL1B and budesonide modestly induced TLR2 mRNA at 6 h with cotreatment revealing a clear *supra*-additivity (Fig. 2B).

To confirm synergy, A549 cells were treated for 6 h with various concentrations of dexamethasone with or without 1 ng/ml IL1B, or with various concentrations of IL1B, with or without 1 μ M dexamethasone. Toll-like receptor 2 mRNA was induced by dexamethasone ($pEC_{50} = 7.4 \pm 0.1$) in a concentration-dependent manner with a maximal effect (E_{Max}) of 3.5-fold (Fig. 2C). In the presence of 1 ng/ml IL1B, which induced TLR2 mRNA by 4.5-fold, the E_{Max} achieved by dexamethasone increased to 31.2-fold. This corresponded to 8.9-fold enhancement over the E_{Max} achieved by dexamethasone alone and occurred without measurable change to the pEC_{50} (Fig. 2C). Similarly, IL1B induced TLR2 mRNA with an E_{Max} of 4.1-fold and a pEC_{50} of 2.04 ± 0.3 (Fig. 2C). Dexamethasone at 1 μ M induced TLR2 mRNA by 3.4-fold, and combination with IL1B concentrations produced an E_{Max} of 29.8-fold with a pEC_{50} of 1.3 ± 0.2 . This represented a 7.3-fold enhancement from the effect of IL1B alone and occurred without significant change in the pEC_{50} (Fig. 2C). These data unequivocally show positive cooperativity between IL1B and dexamethasone leading to substantially increased TLR2 expression without changing the sensitivity to either stimulus.

Proinflammatory cytokines and glucocorticoids enhance TLR2 transcription

To investigate effects on TLR2 transcription, unspliced nuclear RNA (unRNA) was detected using primers spanning the TLR2 intron 2/exon 3 splice junction and used as a surrogate of transcription rate (Fig. S2E). In A549 cells, 2 h of IL1B and dexamethasone treatment induced TLR2 unRNA by

3.4-fold and 2.7-fold, respectively, while cotreatment enhanced this to 11.5-fold (Fig. 2D). Thus, *supra*-additivity at a transcriptional level is confirmed. Following IL1B-plus-dexamethasone cotreatment, TLR2 unRNA was increased 1 h post-stimulation with a maximum at 4 h that preceded the 6 h maximum in TLR2 mRNA (Fig. S2F). From 6 h, reduced TLR2 unRNA levels were consistent with declines in mRNA. Similarly, in pHBECs, IL1B and dexamethasone induced TLR2 unRNA by 17.4 ± 3.6 -fold and 11.1 ± 1.5 -fold, respectively, at 2 h, while IL1B-plus-dexamethasone cotreatment increased this to 95.6 ± 24.0 -fold (Fig. 2E). This effect was significantly greater than the sum of the effects produced by IL1B and dexamethasone alone at 2 h (Fig. 2E, lower panel). Thus, combinatorial enhancements in TLR2 expression by proinflammatory cytokines and glucocorticoids involve *supra*-additivity that occurs at a transcriptional level in the model cell line, A549, and in pHBECs.

TLR2 expression induced by proinflammatory cytokine-plus-glucocorticoid requires NF- κ B and GR

A role for NF- κ B in inducing TLR2 expression was tested using adenoviral-mediated overexpression of I κ B α Δ N, a dominant inhibitor of NF- κ B that lacks the N-terminal region necessary for phosphorylation-induced degradation, thereby efficiently inhibiting NF- κ B in A549 cells (41). IL1B-induced NF- κ B reporter activity in A549 cells showed near maximal inhibition by adenovirus serotype 5 (Ad5)-I κ B α Δ N at a multiplicity of infection (MOI) of 25, whereas the control, Ad5-GFP, had negligible effect (Fig. S3A). NF- κ B reporter cells were infected with Ad5-I κ B α Δ N or Ad5-GFP, each at MOI 25, followed by treatment with IL1B or IL1B-plus-dexamethasone. Western blotting confirmed the expression of GFP and I κ B α Δ N, and luciferase activity induced by IL1B or IL1B-plus-dexamethasone was prevented in the presence of Ad-I κ B α Δ N, but not Ad5-GFP (Fig. 3A). Similar inhibitory effects were found for I κ B α expression, which being an NF- κ B-dependent target also confirms effective inhibition of NF- κ B. Analysis of TLR2 mRNA at 6 h and protein at 8 h showed I κ B α Δ N, but not GFP, overexpression to abolish IL1B- and IL1B-plus-dexamethasone-induced TLR2 expression (Fig. 3A). To provide additional support for a role of the NF- κ B pathway in the induction of TLR2, A549 cells were treated with PS-1145, a selective IKK2 inhibitor (42, 43). Following stimulation with IL1B, NF- κ B reporter activity was reduced by PS-1145 ($pEC_{50} = 5.38$), with E_{Max} achieved at 30 μ M (Fig. S3B). At 30 μ M, PS-1145 significantly, but partially, decreased TLR2 mRNA and protein induced by IL1B-plus-dexamethasone at 6 and 8 h, respectively (Fig. S3C). PS-1145 also reduced IL1B-induced TLR2 mRNA, but had no effect on dexamethasone-induced TLR2 (Fig. S3C). These data support a role for the IKK2-NF- κ B pathway in the induction of TLR2 expression by IL1B and IL1B-plus-dexamethasone.

A549 cells harboring a stably integrated 2 \times GRE-dependent luciferase reporter (A549.2 \times GRE cells) (44) were transfected with GR-targeting or control siRNAs before treatment with

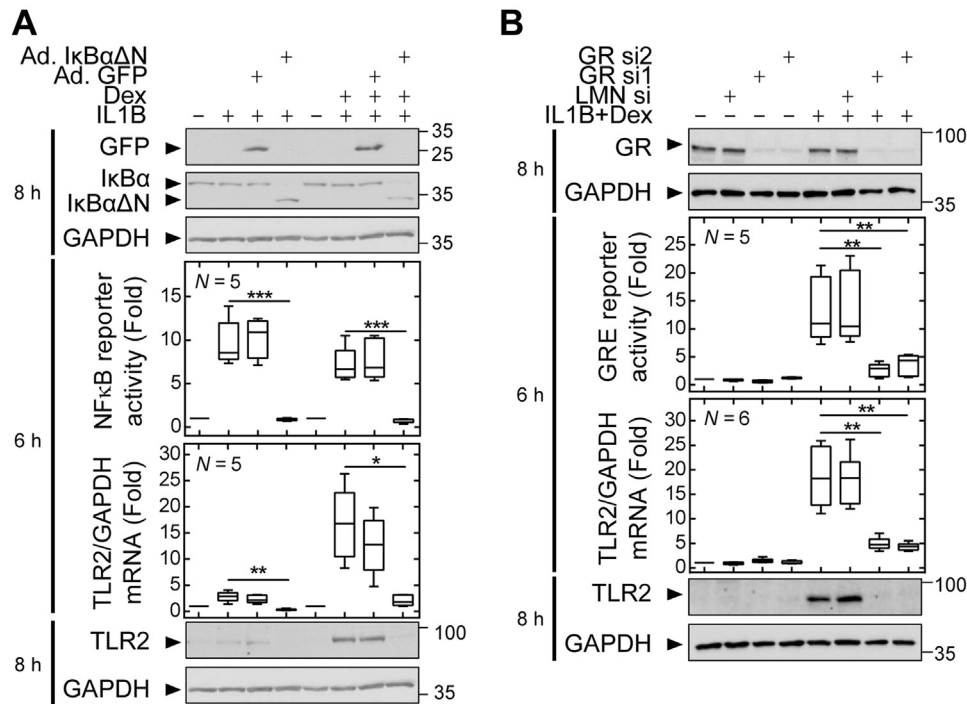


Figure 3. NF-κB and GR are necessary to induce TLR2 expression by proinflammatory cytokines plus glucocorticoid. A, A549 and NF-κB reporter (A549.6κBtk) cells were either not infected, or infected with Ad5-IκBαΔN or Ad5-GFP at an MOI of 25, before treatment with IL1B (1 ng/ml) and/or dexamethasone (Dex; 1 μM). B, A549 and A549.2XGRE cells were incubated with LMNA or GR-specific siRNAs (si1 and si2; 25 nM each) prior to stimulation with IL1B and/or Dex. The cells were harvested for luciferase assay, qPCR, and western blotting at the indicated times. Blots representative of at least five independent experiments (N) are shown. Note, in A, the respective GAPDH blot for GFP and IκBα is also reproduced below TLR2 as these represent sequential reprobing of the same membrane. Luciferase activity and qPCR data of TLR2 normalized to GAPDH were expressed as fold of untreated. Significance was assessed by ANOVA with a Dunnett's post-hoc test. * $p \leq 0.05$, ** $p \leq 0.01$, *** $p \leq 0.001$. Ad5, adenovirus serotype 5; GR, glucocorticoid receptor; GRE, glucocorticoid response element; LMNA, lamin A/C; MOI, multiplicity of infection; NF-κB, nuclear factor-κB; TLR, toll-like receptor.

IL1B-plus-dexamethasone. The two GR-targeting siRNAs strongly suppressed GR protein expression and significantly reduced 2 × GRE reporter activity induced by IL1B-plus-dexamethasone, whereas control siRNA had no effect (Fig. 3B, upper and middle panels). The GR-targeting siRNAs significantly reduced IL1B-plus-dexamethasone-induced TLR2 mRNA and protein levels at 6 and 8 h, respectively (Fig. 3B, lower panels). Control siRNA had no effect, thereby confirming a role for GR in the induction of TLR2 expression by IL1B-plus-dexamethasone.

Effect of proinflammatory cytokines and glucocorticoids on GRE- and NF-κB-dependent transcription

Effects of dexamethasone on the NF-κB pathway were investigated in A549 cells. Phosphorylation of IκBα at Ser32 and Ser36 was induced by IL1B within 2 min, reached a maximum at 5 to 10 min, and was paralleled by complete loss of IκBα by 15 min (Fig. S4A). IL1B also induced Ser536 phosphorylation of p65, which was maximal at 10 to 15 min, while total p65 remained constant (Fig. S4A). There was no effect of dexamethasone cotreatment on IL1B-induced phosphorylation of IκBα or p65 or on loss of IκBα (Fig. S4B). Likewise, dexamethasone modestly decreased NF-κB reporter activity induced by IL1B or TNF (Fig. S4C). Similarly, GRE reporter activity was induced 20.6-fold by dexamethasone, but this was largely unaffected by IL1B or TNF (Fig. S4D). Thus, the effects of dexamethasone on the

NF-κB pathway, or of IL1B/TNF on GRE-dependent transcription, cannot explain synergy occurring at the level of TLR2 expression.

Recruitment of p65 and GR to the TLR2 locus

Recruitment of the NF-κB subunit, p65, and GR to the TLR2 locus was investigated in chromatin immunoprecipitation (ChIP)-seq data from BEAS-2B cells (26). Visualizing these data in the UCSC Genome Browser identified two GR-binding regions, R1 and R2, located ~32 and ~7.3 kb, respectively, upstream of the TLR2 transcription start site (Fig. 4A). Glucocorticoid receptor enrichment at the distal, R1 region was dexamethasone-induced and remained unaffected by TNF as cotreatment in BEAS-2B cells. At the proximal, R2 region, dexamethasone-induced GR enrichment was marginal in BEAS-2B cells, although this was modestly enhanced on TNF cotreatment (Fig. 4A). ChIP-qPCR in A549 cells confirmed increased GR occupancy at R1 following 1 h of budesonide that was unaffected by IL1B cotreatment (Fig. 4B). In pHBECS, GR occupancy at R1 was strongly enhanced by budesonide at 1 h and this was unaffected by IL1B cotreatment (Fig. 4B). At R2, while ChIP-qPCR showed no clear effect of budesonide on GR occupancy at 1 h in A549 cells, IL1B-plus-budesonide modestly increased GR recruitment, an effect that was significant in pHBECS (Fig. 4B).

The ChIP-seq data from Kadiyala *et al.* (26) also shows recruitment of p65 to the R2 region, but not R1, in BEAS-2B

Cytokine and glucocorticoid synergy on TLR2 expression

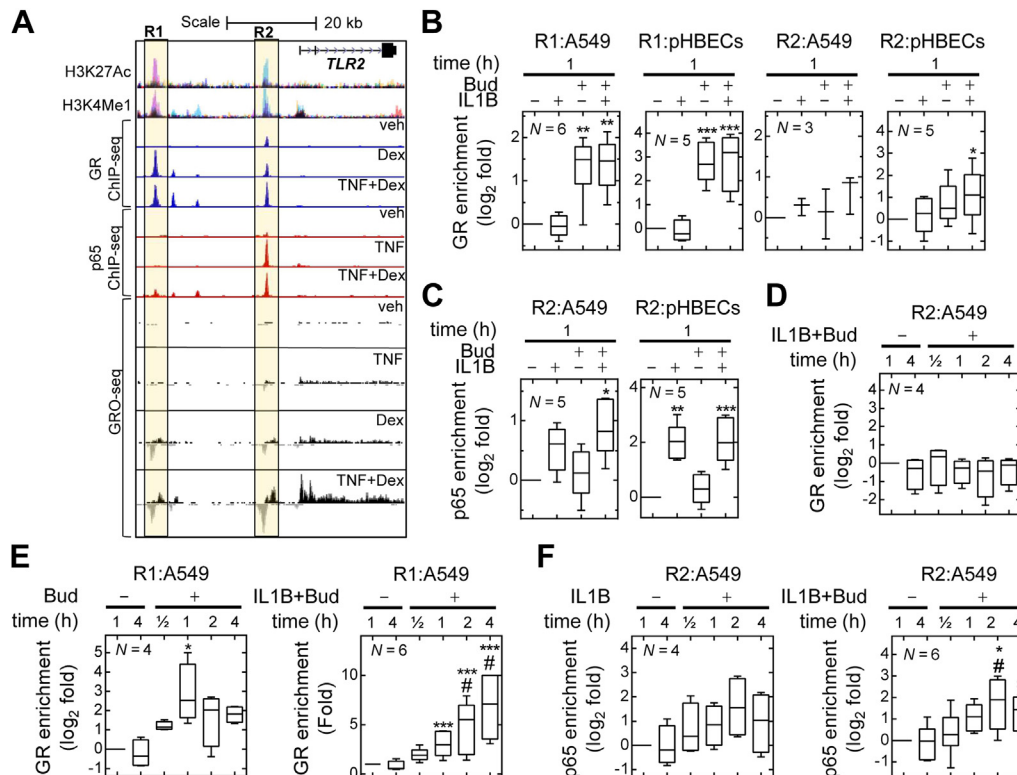


Figure 4. p65 and GR binding and transcriptional activity at *TLR2* locus. A, genome browser snapshot of the *TLR2* gene and ~40 kb upstream of *TLR2* showing histone marks from the ENCODE project (46), ChIP-seq data derived from (26), and GRO-seq data from (45). Regions R1 and R2 are highlighted. GR (blue) and p65 (red) ChIP-seq peaks are shown from BEAS-2B treated with vehicle (veh), dexamethasone (Dex; 100 nM), and/or TNF (20 ng/ml), as indicated. GRO-seq (lower four tracks) shows nascent RNA mapped to the '+' strand (black) or '-' strand (gray) from BEAS-2B cells treated as above for 30 min. B–F, ChIP-qPCR for GR and p65 was performed in A549 and pHBECS either untreated or stimulated with IL1B (1 ng/ml) and/or budesonide (Bud; 300 nM) for 1 h. The data from *N* independent experiments were expressed as log₂ fold enrichment. Significance relative to untreated control (*) or to treated at ½ h (#) was assessed by ANOVA with a Dunnett's post-hoc test. **p* ≤ 0.05, ***p* ≤ 0.01, ****p* ≤ 0.001. ChIP, chromatin immunoprecipitation; GR, glucocorticoid receptor; GRO-seq, global run-on followed by sequencing; pHBEC, primary human bronchial epithelial cell; TLR, toll-like receptor.

cells treated with TNF or TNF-plus-dexamethasone for 1 h (Fig. 4A). In A549 cells, ChIP-qPCR at R2 also suggested increased p65 occupancy following IL1B treatment and this reached significance with IL1B-plus-budesonide (Fig. 4C). More robust effects were apparent in pHBECS, where p65 enrichment at R2 was significant for both IL1B and IL1B-plus-budesonide (Fig. 4C).

Kinetic analysis in A549 cells showed that IL1B alone had no effect on GR enrichment at R1 (not shown). Similarly, at R2, GR recruitment was unaffected by IL1B (not shown) or by IL1B-plus-budesonide (Fig. 4D). Budesonide alone induced GR enrichment at R1 from 30 min that peaked at 1 h and remained elevated until 4 h (Fig. 4E, left panel). IL1B-plus-budesonide cotreatment increased GR enrichment at R1 from 30 min onwards, and this was significantly more at 2 and 4 h relative to 30 min (Fig. 4E, right panel). Similarly, IL1B modestly, but variably, increased p65 enrichment at R2 with an apparent peak from 2 to 4 h (Fig. 4F, left panel). Budesonide alone showed no enrichment of p65 at R2 (data not shown), whereas IL1B-plus-budesonide significantly enhanced p65 enrichment at 2 and 4 h compared to untreated cells (Fig. 4F, right panel). Moreover, p65 enrichment was significantly higher at 2 and 4 h compared to 30 min of IL1B-plus-budesonide treatment.

The above data confirm the recruitment and binding of GR to the R1 region of the *TLR2* locus following glucocorticoid

treatment of A549, BEAS-2B, and pHBECS. Similarly, IL1B or TNF resulted in p65 enrichment at R2 in each of these systems. In each case, these recruitments of GR or p65 were not materially altered by combination treatment.

The p65 and GR-binding regions upstream of the *TLR2* gene drive transcription

Global run-on (GRO)-seq data from BEAS-2B cells treated with TNF and/or dexamethasone for 30 min show bidirectional transcriptional activity, i.e., enhancer RNA (eRNA) production, from the p65- and GR-binding regions, R1 and R2, upstream of the *TLR2* locus (Fig. 4A) (45). Modest increases in nascent RNA production were observed from R1 following stimulation by dexamethasone and TNF-plus-dexamethasone. Similarly, TNF and dexamethasone increased nascent transcripts from R2, and this was enhanced by costimulation. Additionally, cotreatment with TNF-plus-dexamethasone stimulated transcriptional activity throughout the *TLR2* gene. While these data indicate transcriptional activity at R1 and R2, the absence of run-on transcripts from other regions within 50 kb of the *TLR2* locus raise the possibility that R1 and R2 represent the main regions required for *TLR2* upregulation by glucocorticoids and NF-κB-inducing stimuli. As determined by ENCODE (46), these sites coincide with peaks of histone H3 lysine 27 acetylation and lysine 4 methylation,

Cytokine and glucocorticoid synergy on TLR2 expression

which also supports their role as conserved enhancers (Fig. 4A, upper two tracks).

Motif analysis, using the JASPAR CORE database (47, 48), identified three GREs in the R1 region and two p65-binding sites plus one GRE in the R2 region with similarity scores ≥ 300 (Figs. 5A and S5). This corresponds to a p value $\leq 10^{-3}$ and represents significant matching to the respective consensus. To assess their ability to drive transcription, DNA encompassing the three GREs in R1 or the RELA sites and GRE in R2 were cloned separately, or together, into a TATA-containing luciferase reporter prior to transfection into A549 cells and generation of stable lines. In cells harboring the R1-luc reporter, budesonide increased luciferase activity at 6 h with further enhancements at 8 and 24 h (Fig. 5B, left).

Reporter activity from this construct was unaffected by IL1B, whether in the absence or presence of budesonide. For the R2-luc reporter, IL1B increased luciferase activity at 6 h, with further increases apparent until at least 24 h (Fig. 5B, middle). IL1B-plus-budesonide significantly reduced the IL1B-induced luciferase activity at 24 h. For the R1+R2-luc construct, luciferase activity was very modestly but significantly induced by budesonide at 6, 8, and 24 h (Fig. 5B, right). While IL1B alone robustly increased reporter activity, this was markedly enhanced by IL1B-plus-budesonide in a manner that revealed *supra*-additivity (Fig. 5B, lower right).

To explore the contribution of each putative GRE or p65-binding site in driving transcription from R1 and R2, each site was deleted, and stable lines were generated in A549 cells.

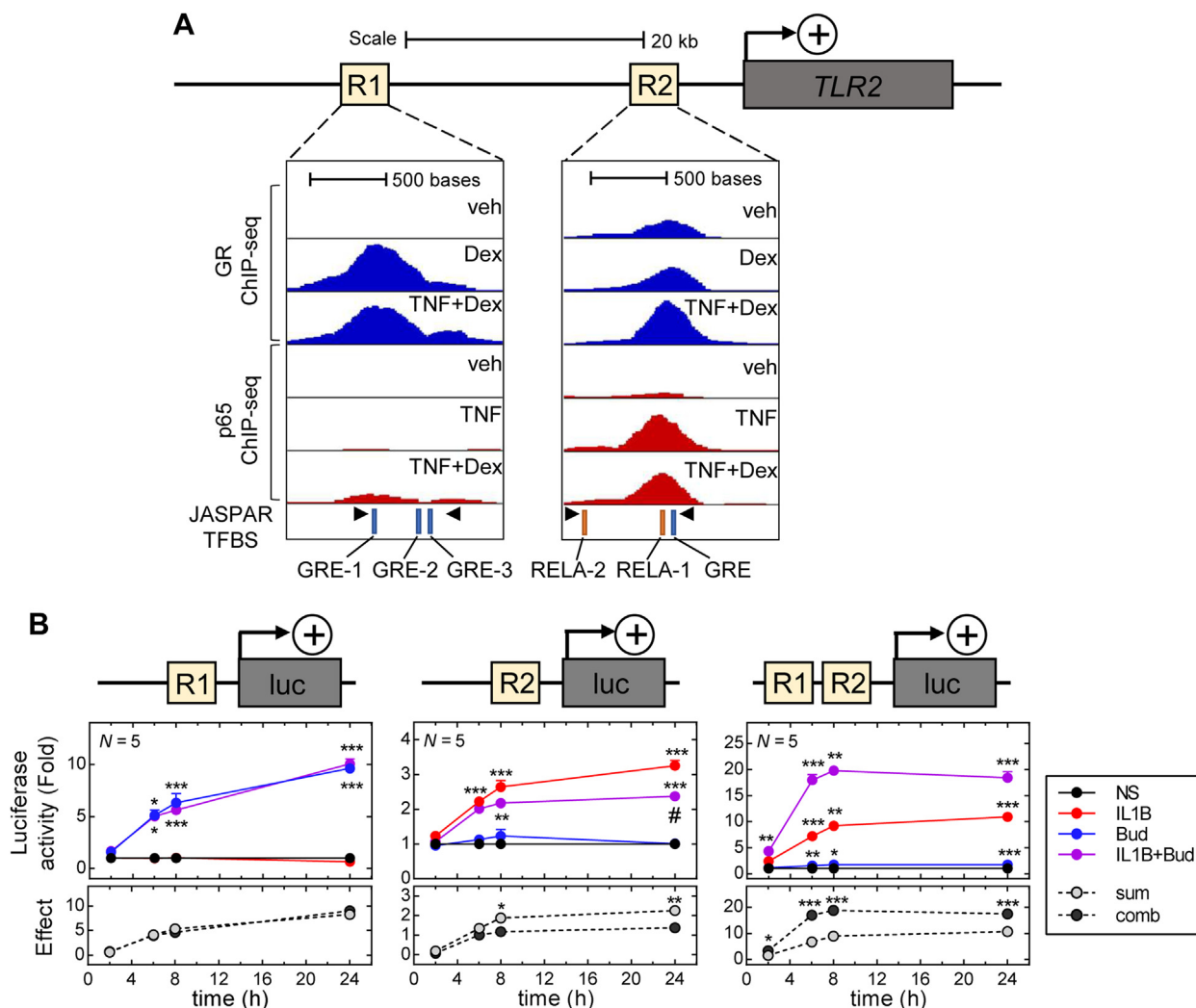


Figure 5. Transcriptional activity from the NF- κ B- and GR-binding regions upstream of TLR2. A, schematic of the TLR2 gene and ~40 kb upstream region showing the GR- and p65-binding regions, R1 and R2, described in Figure 4. Insets show zoomed-in genome browser snapshots for regions R1 and R2 with GR and p65 ChIP-seq traces from BEAS-2B cells treated with vehicle (veh), dexamethasone (Dex; 100 nM), and/or TNF (20 ng/ml), as indicated (data from (26)). GRE- (light blue boxes) and RELA-binding motifs (orange boxes), as predicted from the JASPAR CORE database (score ≥ 300) are highlighted. Black arrowheads represent approximate positions of the primers used to PCR amplify focused regions from R1 and R2 for cloning into a TATA-containing luciferase vector. B, A549 cells stably transfected with empty vector or the R1, R2, or R1 + R2 reporter constructs (shown in the schematics above each graph) were either not treated or treated with IL1B (1 ng/ml) and/or budesonide (Bud; 300 nM) for times indicated followed by luciferase assay. The data from N independent experiments were normalized to empty vector control and plotted as fold of untreated. Significance relative to untreated (*) or IL1B (#; in R2-luc) at each time was assessed by ANOVA with a Dunnett's post-hoc test. Lower panels, the sum effect (i.e., fold - 1) of both treatments (sum) and the effect of combination treatment (comb) is shown. Significance at each time was tested by paired t test. * p ≤ 0.05 , ** p ≤ 0.01 , *** p ≤ 0.001 . ChIP, chromatin immunoprecipitation; GR, glucocorticoid receptor; GRE, glucocorticoid response element; NF- κ B, nuclear factor- κ B; TLR, toll-like receptor.

Cytokine and glucocorticoid synergy on TLR2 expression

Deletion of GRE-1, GRE-2, or GRE-3 in the R1-luc reporter produced partial but significant loss of reporter activity driven by either budenonide or IL1B-plus-budenonide (Fig. 6A). Deletion of all three GREs ablated luciferase activity and supports a role for all three sites in the overall glucocorticoid-mediated transcriptional drive from R1 (Fig. 6A).

In the R2-luc reporter, RELA-1 deletion produced no significant changes in reporter activity induced by either IL1B or IL1B-plus-budenonide (Fig. S6A). Deletion of either RELA-2 or the GRE from the R2-luc reporter significantly enhanced reporter activation by IL1B and IL1B-plus-budenonide (Fig. S6A). Deletion of both RELA-1 and RELA-2 modestly reduced IL1B-induced R2 reporter activity, and IL1B-plus-budenonide-induced reporter activity was significantly, but only marginally, decreased compared to WT (Fig. 6B). However, when the GRE was deleted along with the two RELA sites, no significant change was observed in the IL1B- and IL1B-plus-budenonide-induced luciferase activity compared to the native R2-luc reporter (Fig. 6B). Thus, despite the R2-luc construct showing IL1B-inducibility, classical functional roles for RELA-1, RELA-2, or the GRE were lacking. Rather, negative regulatory functions for factors acting at RELA-2 and the GRE were suggested in the context of IL1B and IL1B-plus-budenonide. Indeed, binding of multiple transcription factors

other than REL proteins are apparent at these sites and thus complexity of transcriptional control is likely (Fig. S6B).

To explore a possible role for NF- κ B, Ad5-I κ B α Δ N was introduced at an MOI of 25 to cause near complete ablation of NF- κ B activity (Fig. S3A). Subsequent treatment with IL1B or IL1B-plus-budenonide induced R2 and R1+R2 reporter activity and this was markedly reduced by I κ B α Δ N (Fig. 6C). Similarly, pretreatment with PS-1145 (30 μ M) significantly decreased IL1B- and IL1B-plus-budenonide-induced activity of the R2-luc and R1+R2-luc reporters (Fig. 6D). Thus, induction of reporter activity by IL1B or IL1B-plus-budenonide requires NF- κ B signaling.

Roles for the GRE and RELA sites in the R1 and R2 regions were interrogated in the context of the combined R1+R2-luc construct. In each case, combined deletion of the three GREs in R1 or/and the two RELA sites and one GRE in R2 significantly attenuated R1+R2 reporter activity by both IL1B and budenonide (Fig. 6E). However, most striking was the substantial loss of IL1B-plus-budenonide-induced reporter activity following these deletions. Not only was R1+R2-luc inducibility by IL1B and budenonide dependent on these sites, but synergy between IL1B and budenonide was completely lost upon deletion of these sites (Fig. 6E). These data strongly implicate a need for both the three GREs in R1 and despite

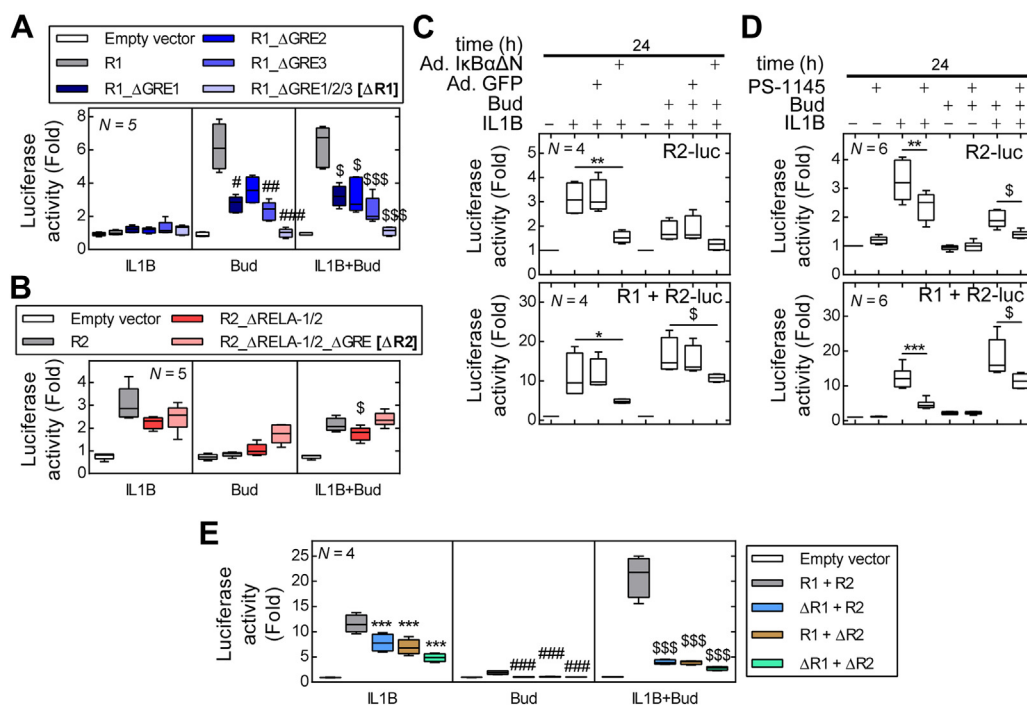


Figure 6. Transcriptional synergy between the GR-binding, R1, and NF- κ B-binding, R2, regions upstream of TLR2. A, A549 cells stably transfected with reporter constructs containing empty vector, wild type R1 (R1), or R1 with the GREs deleted (R1_ΔGRE1, R1_ΔGRE2, R1_ΔGRE3, or R1_ΔGRE1/2/3 [ΔR1]) were either not treated or stimulated with IL1B (1 ng/ml) and/or budenonide (Bud; 300 nM) for 8 h. B, A549 cells stably transfected with reporter constructs containing empty vector, wild type R2 (R2), or R2 with the RELA sites and GREs deleted (R2_ΔRELA-1/2 or R2_ΔRELA-1/2_ΔGRE [ΔR2]) were treated as in A for 24 h. C, A549 cells stably harboring the R2-luc (top panel) or R1+R2-luc (bottom panel) reporter constructs were either not infected or infected with Ad5-I κ B α Δ N or Ad5-GFP at an MOI of 25, before treatment with IL1B and/or Bud for 24 h. D, A549 cells stably harboring the R2-luc (top panel) or R1+R2-luc (bottom panel) reporters were pretreated with PS-1145 (30 μ M) for 90 min followed by the addition of IL1B and/or Bud for 24 h. E, A549 cells stably transfected with reporter constructs containing empty vector, Wild type R1+R2 (R1 + R2), or R1+R2 with GRE and/or RELA sites deleted (ΔR1 + R2, R1 + ΔR2, or ΔR1 + ΔR2). In each case, the cells were harvested for luciferase assay. The data from N independent experiments were expressed as fold of untreated. Significance relative to IL1B (*), Bud (#), or IL1B+Bud (\$) was assessed by ANOVA with a Dunnett's post-hoc test. * $p \leq 0.05$, ** $p \leq 0.01$, *** $p \leq 0.001$. Ad5, adenovirus serotype 5; GR, glucocorticoid receptor; GRE, glucocorticoid response element; MOI, multiplicity of infection; NF- κ B, nuclear factor- κ B; TLR, toll-like receptor.

nonclassical functional roles, RELA-1, RELA-2, and the GRE in R2 in mediating synergy between IL1B and budesonide.

Inhibition of p38 MAPK enhances IL1B-induced TLR2 expression

In A549 cells, IL1B activates the p38, extracellular regulated kinase (ERK), and c-Jun N-terminal kinase (JNK) MAPK pathways, while glucocorticoids reduce MAPK activity (49). Overexpression of DUSP1 inactivates these MAPK pathways but increases IL1B-induced TLR2 mRNA expression (28). This implies a negative role for MAPKs in the regulation of TLR2. To confirm this, A549 cells were pretreated with maximally effective concentrations of SB203580 (10 μM), U0126 (10 μM), and JNK inhibitor VIII (JNK-IN-VIII) (10 μM), which inhibit the p38, ERK, and JNK MAPK pathways, respectively. Following stimulation with IL1B, SB203580 significantly increased IL1B-induced TLR2 mRNA at 6 h, while U0126 and JNK-IN-VIII had no effect (Fig. 7A). As a combination of the three inhibitors produced a similar effect to SB203580 alone, a primary role for p38 MAPK inhibition is suggested. Furthermore, the ability of SB203580 to enhance IL1B-induced TLR2 mRNA expression only starts to become apparent from 2 h onward, before reaching significance at 6 h (Fig. 7B). In

addition, SB203580 enhanced TLR2 mRNA expression in the presence of IL1B, but not in untreated, dexamethasone-treated, or IL1B-plus-dexamethasone-treated cells (Fig. 7C). Thus, the effect of SB203580 is only relevant to the enhancement of TLR2 expression in the context of IL1B treatment. As SB203580, and the combination of SB203580, U0126, and JNK-IN-VIII enhanced IL1B-induced TLR2 unRNA to similar extents at 2 h, an inhibitory effect of p38 MAPK is implicated on TLR2 transcription (Fig. 7D).

In A549 cells, IL1B-induced p38 phosphorylation was maximal at 30 min, before declining by 1 h and thereafter remaining low (Fig. 7E). While dexamethasone had no effect on the initial peak in IL1B-induced p38 phosphorylation, significant inhibition occurred from 1 h onward (Fig. 7E). As the inhibition of p38 MAPK activity by glucocorticoids may contribute to an increase in TLR2 expression, the effect of timing of p38 MAPK inhibition on IL1B-induced TLR2 mRNA was investigated. A549 cells were pretreated, cotreated, or post-treated with SB203580 along with IL1B stimulation prior to analysis of TLR2 mRNA 6 h after the IL1B addition (Fig. 7F). IL1B-induced TLR2 mRNA was significantly enhanced by SB203580 pretreatment and cotreatment. Notably, similar median enhancements of IL1B-induced TLR2 mRNA were achieved with the addition of SB203580 1 h post-

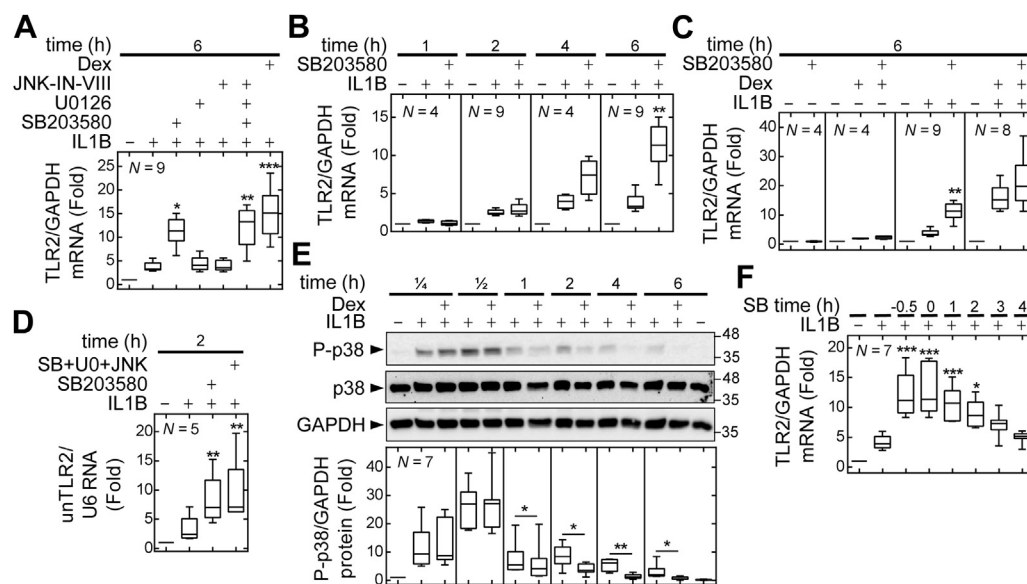


Figure 7. Effect of MAPK inhibition on IL1B- and dexamethasone-induced TLR2 expression. A, A549 cells were either not treated or pretreated with inhibitors of p38 (SB203580), MEK1/2 (U0126), or JNK (JNK-IN-VIII) (each 10 μM), either alone or in combination, for 30 min, followed by addition of IL1B (1 ng/ml) or dexamethasone (Dex; 1 μM), as indicated. The cells were harvested for qPCR analysis at 6 h. TLR2 mRNA data from N independent experiments were normalized to GAPDH and plotted as fold of untreated. Significance relative to IL1B-treated was tested using ANOVA with a Dunnett's post-test. B, A549 cells were either not treated or pretreated with SB203580 for 30 min, followed by addition of IL1B. The cells were harvested for qPCR analysis at the indicated times. TLR2 mRNA data from N independent experiments were normalized to GAPDH and plotted as a fold of untreated at each time point. Significance relative to each time was tested by paired t test. C, A549 cells were either untreated or pretreated with SB203580 for 30 min, followed by addition of IL1B and/or Dex prior to harvesting for qPCR analysis at 6 h. TLR2 mRNA data from N independent experiments were normalized to GAPDH and plotted as fold of untreated at each time point. Significance relative to without SB203580 treatment in each case was tested by paired t test. D, A549 cells were either not treated or pretreated with SB203580 (10 μM) or a combination of SB203580, U0126, and JNK-IN-VIII (SB+U0+JNK; 10 μM each) for 30 min prior to addition of IL1B. After 2 h, the cells were harvested for qPCR analysis. TLR2 unRNA from N independent experiments was normalized to U6 and plotted as fold of untreated. Significance relative to IL1B-treated was tested using ANOVA with a Dunnett's post-test. E, A549 cells were either not treated or stimulated with IL1B and/or Dex prior to harvesting for western blotting at the times indicated. Representative blots of phospho-p38 (P-p38), total p38 (p38), and GAPDH from N independent experiments are shown. Densitometric data for P-p38 was normalized to GAPDH and expressed as fold of untreated control at 15 min. Significance at each time was tested by paired t test. F, A549 cells were either pretreated for 30 min, cotreated, or treated with SB203580 at indicated times after addition of IL1B (SB time). The cells were harvested for qPCR analysis 6 h after IL1B addition. TLR2 data from N independent experiments was normalized to GAPDH and plotted as fold of untreated control. *p ≤ 0.05, **p ≤ 0.01, ***p ≤ 0.001. JNK-IN-VIII, JNK inhibitor VIII; MAPK, mitogen-activated protein kinase; qPCR, quantitative PCR; TLR, toll-like receptor.

Cytokine and glucocorticoid synergy on TLR2 expression

IL1B. However, with longer post-treatment times (>1 h), the ability of SB203580 to enhance TLR2 mRNA expression was progressively lost until by 3 h post-treatment, there was no significant enhancement of IL1B-induced TLR2 mRNA. Thus, the inhibition of IL1B-induced p38 MAPK activity from 1 h onward by dexamethasone overlaps with those times (pre-treatment to 2 h post-treatment) that were necessary for p38 MAPK inhibition to enhance TLR2 mRNA.

p38 α MAPK negatively regulates IL1B-induced TLR2 expression and TLR2 promoter activity

Given selectivity of SB203580 for p38 α and β over p38 δ and γ (Table 1) (50), roles for p38 α and β in the enhancement of IL1B-induced TLR2 expression were investigated. A549 cells were pretreated with the p38 inhibitors, SB203580, BIRB796, and VX745 for 30 min, prior to treatment with IL1B. IL1B-induced phosphorylation of MAPKAPK2, also known as MAPK-activated protein kinase 2 (MK2), a downstream target of p38 α (51), revealed concentration-dependent reductions (pEC₅₀ values = 6.2, 7.9 and 7.8, respectively) by each compound (Figs. 8A and S7A, top panels and Table 1). Likewise, SB203580, BIRB796, and VX745 enhanced IL1B-induced TLR2 mRNA at 6 h (Figs. 8A and S7A, bottom panels), with pEC₅₀ values of 5.85, 7.61, and 6.61 respectively. These were not significantly different from the effects on MK-2 phosphorylation and are therefore consistent with mechanisms that involve p38 α MAPK inhibition (Table 1).

In pHBECS, E_{Max} BIRB796 (100 nM) and VX745 (300 nM) significantly enhanced IL1B-induced TLR2 mRNA at 2 and 6 h (Fig. 8B, top panel), whereas the less selective SB203580 (10 μ M) had no significant effect (data not shown). Likewise, TLR2 unRNA was robustly and significantly enhanced by BIRB796 and VX745 post-IL1B treatment at 2 h, with reduced effects apparent at 6 h (Fig. 8B, bottom panel). Notably, both TLR2 mRNA and unRNA were significantly more induced by IL1B-plus-dexamethasone compared to IL1B in the presence of p38 inhibitors (Table 2). Thus, direct GR-driven transcription of TLR2, along with the inhibitory effect of dexamethasone on p38, may both contribute to the TLR2 expression induced by IL1B-plus-dexamethasone.

To distinguish roles for p38 α and β in regulating TLR2 expression, A549 cells were transfected with either p38 α - or p38 β -targeting siRNAs followed by IL1B treatment. While nontargeting control siRNA had no effect on p38 α , p38 β , or phospho-MK2 protein levels (Fig. S7B), the p38 α -targeting siRNAs reduced p38 α protein expression and IL1B-induced phospho-MK2 (Fig. 8C). There were no effects on p38 β

protein expression, but IL1B-induced TLR2 protein at 8 h was markedly increased by each siRNA (Fig. 8C). Conversely, p38 β -targeting siRNAs reduced p38 β protein and showed no effect on p38 α expression or on IL1B-induced phospho-MK2 protein or IL1B-induced TLR2 expression (Fig. S7, C and D). These effects were reproduced on TLR2 mRNA where IL1B-induced TLR2 mRNA was significantly increased at 6 h in the presence of 1 nM siRNAs targeting p38 α , while control siRNA or p38 β -targeting siRNAs had no effect (Fig. 8D). These data confirm that inhibition of p38 α MAPK leads to increased IL1B-induced TLR2 expression.

A549 cells harboring the TLR2 R1-luc, R2-luc, or R1+R2-luc constructs were transfected with 1 nM p38 α - or p38 β -targeting siRNA pools prior to treatment with IL1B. In R1-luc containing cells, neither the p38 α - nor p38 β -targeting siRNAs had any effect on reporter activity either in the presence or absence of IL1B (Fig. S8A, left panel). With the R2-luc reporter, p38 α -targeting siRNAs significantly increased IL1B-induced reporter activity, while control or p38 β -targeting siRNAs had no effect (Fig. S8A, right panel). With the R1+R2-luc reporter, p38 α -targeting siRNAs significantly increased baseline and IL1B-induced reporter activity (Fig. 8E). In contrast, nontargeting control and p38 β -targeting siRNAs had no effect on baseline or IL1B-induced reporter activity. Similarly, whereas the R1-luc construct was unaffected by the p38 inhibitors (Fig. S8B, left panel), in cells harboring the R2-luc construct, both BIRB796 and VX745 modestly increased IL1B-induced reporter activity at 6, 10, and 24 h (Fig. S8B, middle panel). With the R1+R2-luc reporter cells, BIRB796 and/or VX745 significantly increased IL1B-induced reporter activation at 6, 10, and 24 h (Fig. 8F). Thus, p38 α MAPK acts to dampen IL1B-induced transcriptional activity from these TLR2 reporters.

Since p38 MAPK inhibition enhanced IL1B-induced TLR2, but not baseline-, dexamethasone-, or IL1B-plus-dexamethasone-induced TLR2 mRNA (Fig. 7C), the effects of p38 MAPK inhibition were examined on IL1B-induced recruitment of p65 to the TLR2 promoter (Fig. 8G). However, no obvious effect of BIRB796 was apparent on the recruitment of p65 to the R2 region at either 2 or 4 h post-IL1B treatment. Similarly, dexamethasone was also without effect at these same times (Fig. 8G). Indeed, combining these data with those from Figure 4F confirms no overall effect ($N = 7$) of glucocorticoid on the recruitment of p65 by IL1B to R2 (Fig. S9). Despite this, p38 MAPK phosphorylation was significantly reduced by glucocorticoid at both 2 and 4 h (Fig. 7E). These data do not, therefore, support an effect of p38 MAPK inhibition, whether due to direct kinase inhibition or the effects of glucocorticoid, on the recruitment of p65 to the R2 region of TLR2.

Table 1
Selectivity of SB203580, BIRB796, and VX745 for p38 α / β / δ / γ

MAPK inhibitor	pEC ₅₀		p value	pK _i			
	p-MK2 reduction	TLR2 enhancement		p38 α	p38 β	p38 δ	p38 γ
SB203580	6.2±0.25	5.85±0.28	0.4375	7.92	7.15	5	5.82
BIRB796	7.94±0.21	7.61±0.18	0.0625	9.35	8.14	7.11	8.54
VX745	7.79±0.30	6.61±0.29	0.0625	8.55	6.8	5	5

pEC₅₀ values of the three p38 inhibitors on p-MK2 reduction and TLR2 mRNA enhancement in IL1B-treated A549 cells are shown (related to Figs. 8A and S7A). The pK_i values of the inhibitors on the p38 isoforms were derived from Davis *et al.* (50).

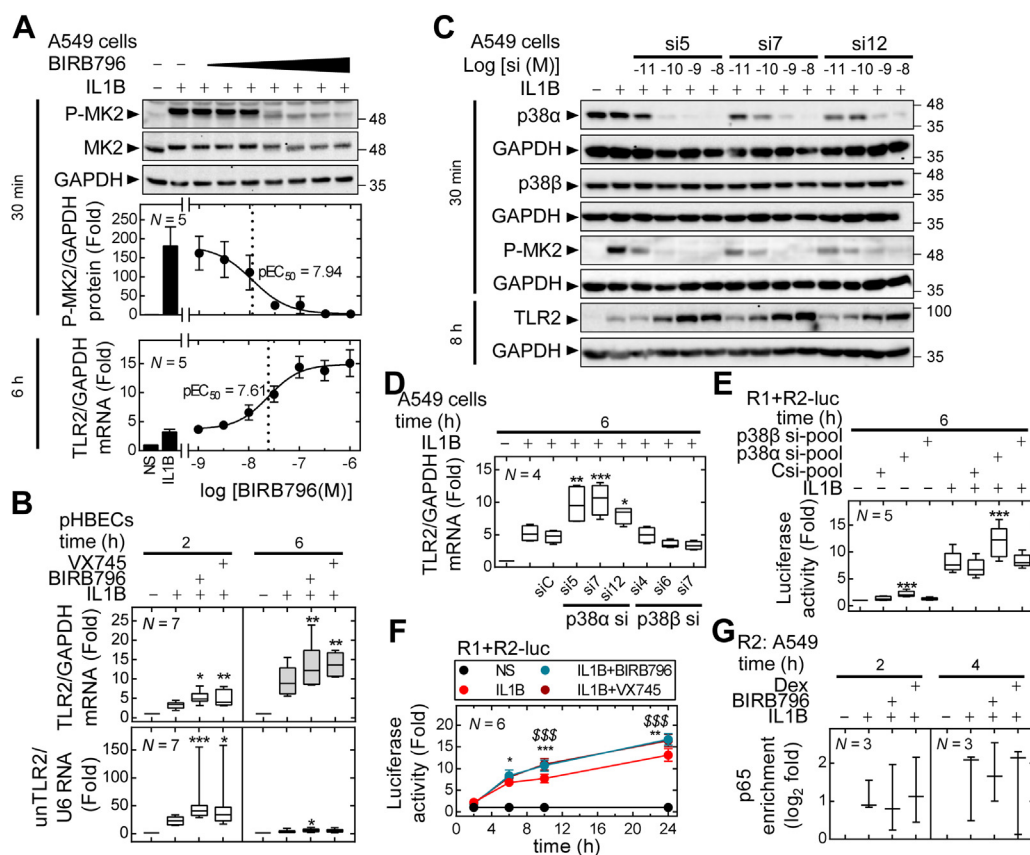


Figure 8. p38 α MAPK inhibition upregulates IL1B-induced TLR2 expression and R1+R2-reporter activity. A, A549 cells were either not treated or pretreated with BIRB796 at various concentrations for 30 min prior to stimulation with IL1B (1 ng/ml). The cells were harvested at 30 min for Western blot analysis and 6 h for qPCR analysis. Blots representative of *N* independent experiments for phospho-MK2 (P-MK2), total MK2 (MK2), and GAPDH are shown. Densitometric data for P-MK2 and TLR2 mRNA, each normalized to GAPDH, were plotted as fold relative to untreated. B, pHBECs grown in submersion culture were either not stimulated or pretreated with BIRB796 (100 nM) or VX745 (300 nM) for 30 min, followed by addition of IL1B. The cells were harvested for qPCR analysis at 2 and 6 h. Upper panel, TLR2 mRNA was normalized to GAPDH and (lower panel) TLR2 unRNA was normalized to U6. In each case, data from *N* independent experiments were expressed as fold relative to untreated control. C, A549 cells were incubated with concentrations of p38 α siRNAs (*si5*, *si7*, and *si12*) as indicated, prior to addition of IL1B. The cells were harvested after 30 min and 8 h for western blot analysis. Blots representative of at least four independent experiments are shown. D, A549 cells were incubated with either control siRNA (*siC*), p38 α siRNAs (*si5*, *si7*, and *si12*), or p38 β siRNAs (*si4*, *si6*, and *si7*), each at 1 nM, followed by treatment with IL1B. The cells were harvested at 6 h for qPCR analysis. TLR2 mRNA data from *N* independent experiments was normalized to GAPDH and expressed as fold of untreated. A549 cells stably harboring the R1+R2-luc reporter were either (E) incubated with pools of the p38 α or p38 β siRNAs used in C and D (1 nM) or (F) pretreated with BIRB796 (100 nM) or VX745 (300 nM) for 30 min, followed by treatment with IL1B. The cells were harvested for luciferase assay at indicated times. Luciferase activity from *N* independent experiments was expressed as fold relative to untreated. In B, D, E, and F, significance relative to IL1B was tested by ANOVA with a Dunnett's post-hoc test. In F, * and \$ represent significance of IL1B+BIRB796 and IL1B+VX745, respectively, relative to IL1B. G, A549 cells were either not treated or pretreated with BIRB796 (100 nM) for 30 min, followed by addition of IL1B and/or dexamethasone (Dex; 1 μ M). The cells were harvested at the indicated times, and ChIP-qPCR for p65 was performed. Data from *N* independent experiments were plotted as log₂ fold enrichment. **p* \leq 0.05, ***p* \leq 0.01, ****p* \leq 0.001. ChIP, chromatin immunoprecipitation; MAPK, mitogen-activated protein kinase; pHBEC, primary human bronchial epithelial cell; qPCR, quantitative PCR; TLR, toll-like receptor.

Proinflammatory signaling by IL1B-plus-dexamethasone-induced TLR2

To explore the functionality of TLR2 expression that was induced by IL1B-plus-glucocorticoid, A549 cells were pretreated with IL1B-plus-dexamethasone for 24 h to induce

TLR2 expression. The medium was then changed to serum-free medium containing the Ad5-NF- κ B.luc vector for 14 h, to allow the analysis of NF- κ B-dependent reporter activity. After changing to fresh serum-free medium, the cells were either not stimulated or were stimulated for 6 h with the TLR2

Table 2
Fold differences between IL1B+MAPK inhibitor and IL1B-plus-dexamethasone-induced TLR2 mRNA and unRNA

Time (h)	mRNA				unRNA			
	IL1B	IL1B+BIRB796	IL1B+VX745	IL1B+Dex	IL1B	IL1B+BIRB796	IL1B+VX745	IL1B+Dex
2	3.32 \pm 0.44	5.08 \pm 0.84*	4.45 \pm 0.93**	7.24 \pm 1.49	22.24 \pm 3.47	58.92 \pm 24.16**	50.97 \pm 26.87	103.83 \pm 48.60
6	8.924 \pm 1.21	12.54 \pm 1.40***	13.71 \pm 1.14***	30.81 \pm 3.263	2.72 \pm 0.61	5.52 \pm 1.01***	4.11 \pm 1.06***	24.44 \pm 4.95

Primary human bronchial epithelial cells were either untreated or pretreated with BIRB796 (100 nM) or VX745 (300 nM) for 30 min prior to the addition of IL1B (1 ng/ml) and/or dexamethasone (Dex; 1 μ M). The cells were harvested for qPCR analysis of mRNA and unRNA at 2 and 6 h. TLR2 mRNA was normalized to GAPDH, and TLR2 unRNA was normalized to U6. Data from 5 independent experiments are shown as fold relative to untreated. * = comparison with IL1B+Dex (ANOVA with a Dunnett's post-test). **p* \leq 0.05, ***p* \leq 0.01, ****p* \leq 0.001.

Cytokine and glucocorticoid synergy on TLR2 expression

agonists, Pam2CSK4 and Pam3CSK4 (52, 53), prior to luciferase assay (See Fig. S10A for a schematic of the experimental protocol). Cells that were not pretreated and those that were pretreated with IL1B-plus-dexamethasone, but then not further stimulated, showed only very low levels of NF- κ B activity. However, stimulation with Pam2CSK4 and Pam3CSK4 increased NF- κ B reporter activity in a concentration-dependent manner (pEC₅₀ values = 8.51 and 6.0, respectively) (Fig. 9A). Using a similar experimental approach (Fig. S10A), A549 cells harboring an interferon regulatory factor 1 (IRF1)-driven luciferase reporter were either not pretreated or pretreated with IL1B-plus-dexamethasone for 24 h to induce TLR2 expression prior to incubating in serum-free medium for 14 h. After a further change to fresh serum-free medium, the cells were either not stimulated or treated with Pam2CSK4 and Pam3CSK4 (Fig. 9B). Relative to no

pretreatment, the IL1B-plus-dexamethasone pretreated cells revealed a modestly, ~2-fold, elevated level of luciferase activity. This showed further concentration-dependent increases in response to Pam2CSK4 and Pam3CSK4 (pEC₅₀ values = 9.09 and 6.05, respectively) (Fig. 9B). Thus, Pam2CSK4 and Pam3CSK4 induce activation of NF- κ B- and IRF1-dependent reporter activity in IL1B-plus-dexamethasone-treated A549 cells.

To confirm roles for TLR2 in the NF- κ B- and IRF1-induced activity in IL1B-plus-dexamethasone pretreated cells, silencing of TLR2 was performed in A549 cells and pHBECS prior to stimulation with Pam2CSK4 and Pam3CSK4. While non-targeting control siRNAs had no effect on IL1B-plus-dexamethasone-induced TLR2 expression, TLR2-targeting siRNAs substantially reduced TLR2 protein expression in both A549 cells (Figs. 9C and S10, B and C) and pHBECS (Fig. 9D).

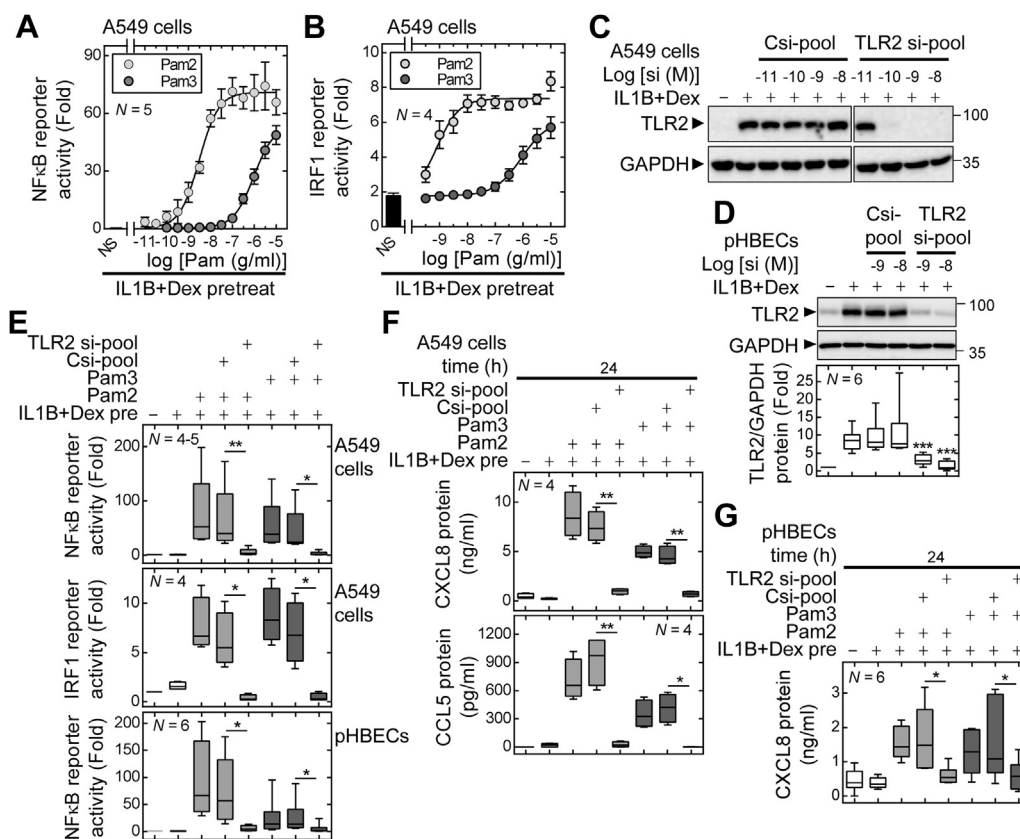


Figure 9. Proinflammatory signaling following agonism of IL1B plus dexamethasone-induced TLR2. A, A549 cells were either not pretreated or pretreated with IL1B (1 ng/ml) plus dexamethasone (Dex; 1 μ M) for 24 h to induce TLR2. Ad5-NF- κ B.luc reporter was added in serum-free medium (SFM) for 14 h prior to either no stimulation (NS) or stimulation for 6 h with Pam2CSK4 (Pam2) and Pam3CSK4 (Pam3) at the indicated concentrations. See Fig. S9A for experimental design. B, IRF1 reporter (A549.6 \times IRF1.luc) cells were treated as in A except that SFM alone was added (instead of Ad5-NF- κ B.luc) and the cells were harvested 8 h after stimulation with Pam2 and Pam3. In (A) and (B), luciferase activity from *N* independent experiments was expressed as fold of cells with no pretreatment. C, A549 cells, or D, pHBECS grown in submersion culture, were incubated with pools of either control siRNAs or TLR2 siRNAs (1 nM each) prior to addition of IL1B plus Dex for 24 h. The cells were incubated in SFM for 14 h prior to harvesting for Western blot analysis. Blots representative of six independent experiments (*N*) are shown. Note, the siRNA controls shown in C also appear in Fig. S10B. (D - lower panel) following densitometric analysis, the data for TLR2 were normalized to GAPDH and plotted as fold of untreated. Significance relative to IL1B plus Dex treatment was assessed using ANOVA with a Dunnett's post-test. E, A549 cells (top panel), IRF1 reporter (A549.6 \times IRF1.luc) cells (middle panel), or pHBECS grown in submersion culture (lower panel) were incubated with pools of control siRNAs or TLR2 siRNAs (1 nM each) prior to stimulation with IL1B plus Dex (IL1B+Dex pre) to induced TLR2 expression. After 14 h in SFM + Ad5.NF- κ B.luc, or SFM (for IRF1 reporter cells), the cells were stimulated with Pam2 (100 ng/ml) or Pam3 (10 μ g/ml). The cells were harvested after 6 h (top and bottom panels) or 8 h (middle panel) for luciferase assay. Data from *N* independent experiments were expressed as fold of untreated control. F, A549 cells, or G, pHBECS in submersion culture, were treated as in E, prior to stimulation with Pam2 (100 ng/ml) or Pam3 (10 μ g/ml). After 24 h, supernatants were collected for analysis of CXCL8 and CCL5 protein by ELISA. Data from *N* independent experiments were plotted as chemokine release. Significance in E-G was tested by paired *t* test. **p* \leq 0.05, ***p* \leq 0.01, ****p* \leq 0.001. Ad5, adenovirus serotype 5; NF- κ B, nuclear factor- κ B; pHBEC, primary human bronchial epithelial cell; TLR, toll-like receptor.

The ability of Pam2CSK4 and Pam3CSK4 to induce NF- κ B and IRF1 reporter activity in IL1B-plus-dexamethasone pretreated A549 cells, or pHBECS, was unaffected by the control siRNAs but essentially abolished by TLR2-targeting siRNAs (Fig. 9, E and F). In IL1B-plus-dexamethasone pretreated A549 cells, Pam2CSK4 and Pam3CSK4 both induced release of CXCL8 and CCL5 (Fig. 9F). In each case, this response was prevented by the TLR2-targeting siRNAs, but not affected by control siRNA (Fig. 9F). Similar results were obtained for CXCL8 in pHBECS (Fig. 9G). CCL5 release from pHBECS was below the detection limit of the ELISA (data not shown). Taken together, these data show that TLR2, when induced by IL1B-plus-dexamethasone, drives proinflammatory responses that include activation of NF- κ B and IRF1 and the release of inflammatory chemokines.

Discussion

Glucocorticoid therapies represent an effective means to reduce the inflammation that drives many chronic inflammatory diseases, including asthma. However, a growing body of literature suggests that glucocorticoids can also induce proinflammatory effects (54, 55). While these may variously promote, or help spare, host defense mechanisms in the context of an otherwise anti-inflammatory glucocorticoid (56), the underlying molecular mechanisms remain poorly characterized. Examples of glucocorticoid-induced proinflammatory responses include NLRP3 inflammasome-mediated sensitization with the release of proinflammatory cytokines (57) and upregulation of cytokine-induced TLR2 (30, 31, 58–63). Thus, in pulmonary epithelial cells, the addition of dexamethasone to nontypeable *Haemophilus influenzae* or TNF-plus-interferon γ as stimuli further increased TLR2 expression (30, 58, 59). Moreover, inhalation of a clinically accepted high dose of budesonide by healthy male volunteers induced TLR2 expression in bronchial biopsies and peripheral blood (17). The current analysis expands on these findings to clearly document synergistic upregulation of TLR2 expression by inflammatory cytokines and glucocorticoids in epithelial cell lines (A549, BEAS-2B) and in pHBECS grown as undifferentiated submersion culture or as highly differentiated ALI cultures. In each system, modest induction of TLR2 expression by E_{Max} concentrations of IL1B, TNF, or glucocorticoid resulted in robust *supra*-additive effects on TLR2 expression when either cytokine was combined with glucocorticoid. This synergy also occurred for TLR2 unRNA and suggests mechanisms operating at the level of transcription.

Molecular and pharmacological interventions demonstrated that the induction of TLR2 expression by inflammatory cytokine-plus-glucocorticoid required both NF- κ B and GR. However, while IL1B- and IL1B-plus-dexamethasone-induced TLR2 expression was prevented by a dominant inhibitor of NF- κ B, the partial (~50%) reduction in TLR2 expression produced by a selective IKK2 inhibitor suggests contributions from additional IKK2-independent pathways. Furthermore, glucocorticoids showed little effect on NF- κ B-dependent reporter activation (or on upstream pathways), while

inflammatory stimuli modestly reduced GRE reporter activity. Thus, the mechanisms of cooperativity are unlikely to be mediated *via* simple effects on each core pathway. This is borne out by ChIP analysis of two novel NF- κ B/p65 and GR-binding regions, R1 and R2, located ~32 and ~7.3 kb upstream respectively, of the *TLR2* transcription start site. In response to glucocorticoid, robust GR binding primarily to the distal R1 region was shown in A549 and BEAS-2B cells as well as in pHBECS. This pattern was similar to that in data from a prior ChIP-seq analysis of dexamethasone-treated A549 cells in which modest GR binding to R1 and no GR enrichment at the R2 region was shown (64). At 1 h, this recruitment of GR was unaffected by cotreatment of glucocorticoid with IL1B or TNF. Similarly, p65 binding at the proximal R2 region, in response to IL1B or TNF treatment, was not further altered by cotreatment with glucocorticoid. Thus, the delivery of GR or p65 to R1 or R2, respectively, does not account for cytokine/glucocorticoid synergy on TLR2 expression (Fig. 10A).

As GRO-seq data from cytokine- and glucocorticoid-stimulated BEAS-2B cells revealed enhancer RNA transcription, primarily from R1 and R2, critical roles for these two regions in promoting TLR2 expression were suggested. This concept is supported by the histone modifications, H3K27Ac and H3K4Me1, which often mark active enhancers (65, 66), being present at R1 and R2, but not elsewhere in the vicinity of the *TLR2* locus. Indeed, cloning of the R1 region revealed glucocorticoid-inducible transcription due to three simple GREs. Likewise, motif analysis identified two putative p65-binding sequences and a GRE in the R2 region. This region also drove cytokine-inducible transcriptional activity that was prevented by inhibition of NF- κ B. Despite this, the deletion of these sites in R2 showed minimal effect on IL1B-induced transcription and suggests that additional sites might be important. Indeed, the enrichment of p65 at R2 was relatively weak, relative to sites in highly cytokine-induced genes, such as *TNF* or *CXCL8* (data not shown). This questions whether direct binding of p65 to R2 is the only, or even, a main, driver of TLR2 synergy. For example, additional factors, even including other NF- κ B subunits, could play contributing roles. However, the R1 reporter showed glucocorticoid-inducibility that was unaffected by IL1B, while budesonide repressed the IL1B-induced R2 reporter. Nevertheless, juxtaposing R1 and R2 resulted in IL1B- and modest budesonide-induced transcription that was synergistically increased by IL1B-plus-budesonide. Importantly, loss of the three GRE sites in R1 and/or the p65 and GRE sites in R2 prevented this synergy. Thus, essential roles for these sites in regulating *TLR2* transcription are indicated.

Taken together, our results support positive cooperative effects between the GR and NF- κ B pathways acting *via* distinct and distantly located genomic regions upstream of *TLR2* (Fig. 10, A and B). Superficially, similar effects were suggested for the mouse *TLR2* promoter (29). However, this study involved only <1.5 kb of upstream DNA and is therefore not reflective of the more distal binding of GR and p65 to R1 and R2, which are ~32 and ~7.3 kb upstream of the human *TLR2* locus. This illustrates why studies using human *TLR2* are

Cytokine and glucocorticoid synergy on TLR2 expression

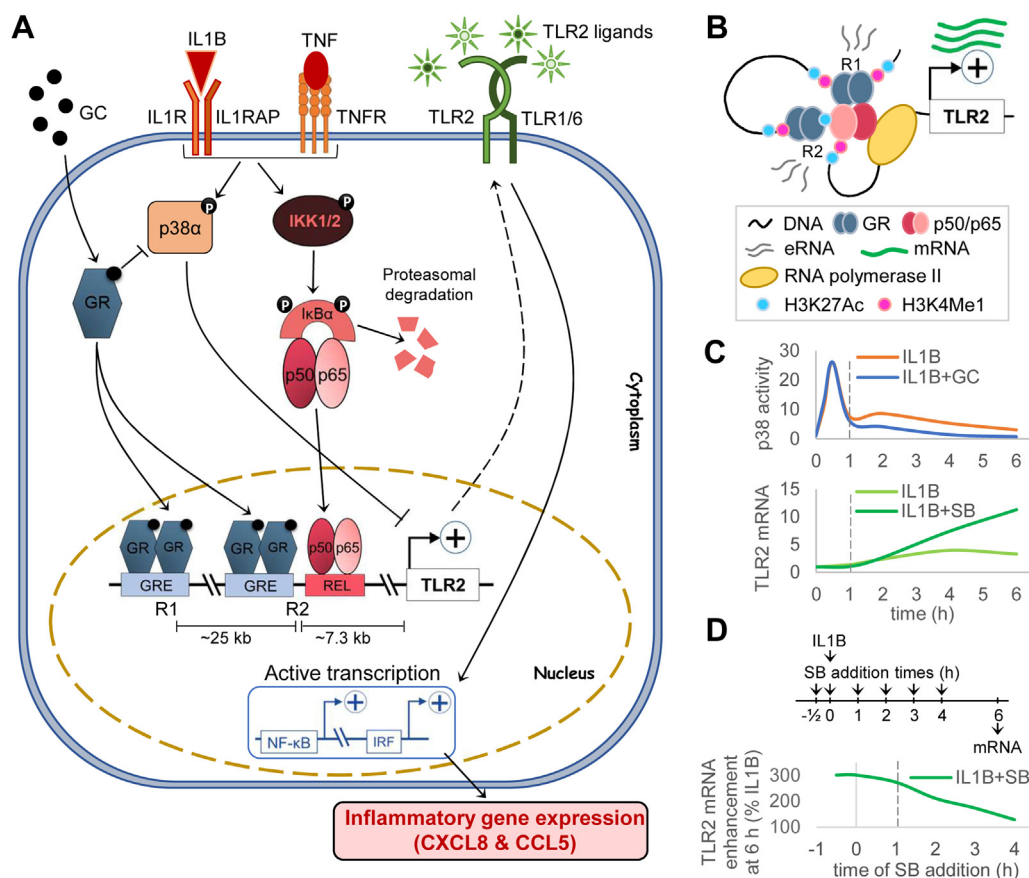


Figure 10. Model for synergy between proinflammatory cytokines and glucocorticoid on TLR2 expression. **A**, the proinflammatory cytokines, IL1B and TNF, activate NF- κ B signaling through their receptors, IL1R/IL1RAP and TNFR, respectively. This leads to the recruitment of NF- κ B (p50/p65) to RELA sites in the R2 region upstream of the TLR2 transcription start site. IL1B and TNF also activate p38 MAPK. As shown by small molecule inhibitors and silencing, this negatively regulates TLR2 transcription *via* an effect that occurs downstream of binding of p65 to R2. Glucocorticoid (GC) binds to cytoplasmic glucocorticoid receptor (GR). This translocates to the nucleus and primarily binds GREs in the R1 region and to a lesser extent in the R2 region upstream of the TLR2 gene. GCs only modestly induce TLR2 expression. However, in the presence of IL1B or TNF, GR and NF- κ B cooperate to increase transcription from the TLR2 gene. In addition, GCs inactivate p38 MAPK *via* a variety of mechanisms (not shown). This switches off the p38 MAPK-dependent feed-forward control loop and enables enhanced transcription of TLR2. These events combine to synergistically induce TLR2 expression following cotreatment with IL1B/TNF and a GC. Functionally, the TLR2 ligands, Pam2CSK4 and Pam3CSK4, act on TLR2 (presumably localized in the cell membrane; *dotted line*) to induce NF- κ B and IRF-dependent transcription (note that in each case, the specific factors involved were not identified and are not shown). The release of inflammatory chemokines, such as, CXCL8 and CCL5, is also increased following the agonism of TLR2. **B**, a proposed model for the genomic events leading to enhanced TLR2 gene transcription is shown. Positive cooperative interaction between GR and p50/p65 may occur *via* looping between distantly located DNA elements, R1 and R2, upstream to the TLR2 gene. Such events can bring GR and p50/p65 in close proximity. These can then act together to enhance TLR2 transcription by RNA polymerase II. **C**, *upper graph*, delayed inhibition of p38 MAPK by GC (from 1 h onwards; *dotted line*) is depicted in A549 cells. *Lower graph*, effect of SB203580 (SB), a p38 inhibitor, on IL1B-induced TLR2 mRNA in A549 cells over time is shown. *Upper and lower graphs* are adapted from Figure 7, B and E, respectively. **D**, enhancement of IL1B-induced TLR2 mRNA expression by SB203580 when added at different times pre- and post-IL1B. A schematic shows the addition of SB203580 relative to IL1B addition and the graph is adapted from Figure 7F. Progressive loss of the ability of SB203580 to enhance IL1B-induced TLR2 mRNA, when added 1 h after IL1B treatment indicates that p38 inhibition occurring at \sim 1 h (either by SB203580 or by GC) is essential to enhance cytokine-driven TLR2 expression. GRE, glucocorticoid response element; MAPK, mitogen-activated protein kinase; NF- κ B, nuclear factor- κ B; TLR, toll-like receptor.

necessary to unravel mechanistic effects relevant to synergy in human epithelial cells. Such mechanisms might include DNA looping between R1 and R2 to allow interaction between these distant, but active, enhancer regions. Indeed, H3K4Me1 is suggested to play a role in recruiting chromatin remodeling complexes into enhancers, while H3K27Ac may help with eRNA production (67, 68). Furthermore, eRNAs, as observed for R1 and R2, may promote RNA pol II recruitment (69, 70) as well as interactions between enhancers and promoters *via* DNA looping (71, 72). Certainly, DNA looping can occur between GR-binding sites that cluster near many glucocorticoid-responsive gene loci (73). Indeed, the modest enrichment of GR observed at the p65-binding R2 region upon co-treatment

with IL1B-plus-budesonide may be indicative of looping, and such interactions could enable cooperation between R1 and R2 to synergistically drive *TLR2* gene expression. Similar looping mechanisms are suggested for GR/AP-1 interactions that promote synergistic activation of transcription from GREs (74). Likewise, physical interactions between GR and p65 are well-established (75). Thus, DNA looping to enable interaction between GR at R1 and p65 at R2 could contribute to synergy on TLR2 expression (Fig. 10B). Indeed, juxtaposition of GREs and NF- κ B-binding sites in reporter constructs can produce transcriptional synergy (24). Similar GR/NF- κ B interactions are also implicated in the cooperative effects between glucocorticoid and cytokines at multiple loci (25, 26), including anti-

inflammatory genes (14, 27). While other mechanisms of synergy might include the ability of one factor to enhance binding by the other, as is described for pioneer factors (76), the enrichment of p65 by IL1B at R2 was not materially altered with IL1B-plus-glucocorticoid at 1, 2, or 4 h. However, despite budesonide-induced GR binding at R1 being relatively unaffected at 1 h by costimulation, GR enrichment showed persistent time-dependent increases with IL1B-plus-budesonide cotreatment. Thus, time-dependent enhancement of GR recruitment to the *TLR2* locus may possibly contribute to transcriptional synergy. This requires further examination, particularly in the context of DNA looping and possible changes to the chromatin environment.

A further mechanism contributing to cytokine/glucocorticoid synergy is the regulation of TLR2 expression by p38 MAPK. Unlike many inflammatory genes, where MAPKs positively regulate transcription, mRNA stability, or translation (77), TLR2 expression is negatively regulated by p38 MAPK. Thus, overexpression of the MAPK phosphatase, DUSP1, reduces activity of all MAPKs but enhances TLR2 expression in response to proinflammatory stimuli, including IL1B in A549 cells (28, 31, 58). Likewise, p38 inhibitors enhance TLR2 expression in the context of IL1B and our analysis of TLR2 unRNA indicates this to be transcriptional. Furthermore, the effect was also apparent in pHBECS and this suggests physiological relevance. In terms of mechanism, IL1B-induced activation of the R1+R2 reporters was also enhanced by p38 inhibition. However, this effect was considerably reduced compared to the enhancement of TLR2 expression. Thus, the reporters may lack some components, for example other DNA-binding regions, necessary to fully capture the negative regulation by p38 MAPK. Using selective p38 α inhibitors and siRNAs, we report, for the first time, a role for p38 α , but not p38 β , in the negative regulation of TLR2 expression in A549 cells. In addition, the delayed timing of p38 MAPK inhibition by dexamethasone, i.e., from 1 h onwards, coincides with the times when TLR2 mRNA expression becomes enhanced following inhibition of p38 MAPK (Fig. 10C). Furthermore, addition of p38 inhibitors 1 h after IL1B addition retained the ability to enhance TLR2 mRNA expression, whereas further delay in p38 MAPK inhibition progressively reduced the ability to enhance TLR2 mRNA expression (Fig. 10D). Thus, inhibition of the rapid activation of p38 MAPK by IL1B, which peaks at \sim 30 min, but is greatly reduced by 1 h, was not necessary to enhance TLR2 expression. However, inhibition of p38 MAPK activity occurring after 1 h appeared essential for the enhancement of TLR2 mRNA expression. This timeframe coincides with when glucocorticoids both inhibit p38 MAPK and enhance TLR2 mRNA expression. Thus, it is the relatively low levels of p38 MAPK activity, occurring from 1 h post-IL1B stimulation, which are responsible for restricting TLR2 expression. Equally, the loss of p38 MAPK activity at these times due to inhibition of p38 MAPK by kinase inhibitors or glucocorticoids promotes TLR2 expression (Fig. 10, C and D). This novel regulatory framework means that the inhibition of MAPKs by glucocorticoids can yield divergent effects on gene expression. Glucocorticoids will

reduce IL1B-induced expression of numerous inflammatory genes that require MAPK activity (28, 49, 78), whereas the expression of TLR2, and certain other genes (23), will be simultaneously enhanced. These modulatory effects on inflammatory gene expression are not only underappreciated but are likely to be fundamentally important to understanding inflammatory events that resist repression by glucocorticoids.

Mechanistically, the above data point to a delayed effect of the p38 MAPK pathway in restricting the expression of TLR2 when induced by inflammatory stimuli. What mediates this effect is currently unclear, but clues may be gained from the current data. Inhibition of p38 MAPK enhanced IL1B-induced TLR2 mRNA, but not basal TLR2 mRNA, or following either glucocorticoid treatment or glucocorticoid-plus-IL1B, where p38 MAPK will have been repressed by the glucocorticoid. Thus, the restrictive effects of p38 MAPK operate primarily on IL1B-induced pathways rather than on those mediated by the glucocorticoid. In this regard, p38 MAPK inhibition produced no obvious effect on the recruitment of p65 to R2, and indeed, p38 MAPK inhibition is most generally associated with reduced NF- κ B activity (77). However, MAPKs may play active roles in the switching off of transcription factors (79, 80). For example, the inactivation of ELK1 has been shown to involve a MAPK-dependent SUMOylation event (81). Similarly, SB203580 can promote expression of the acute phase transcription factor, c-fos (82). We therefore hypothesize the existence of factors that are negatively regulated by p38 MAPK and which are important for the upregulation of TLR2. Interestingly, blockade of protein synthesis, using cycloheximide, upregulates IL1B-induced TLR2 mRNA in a manner that is not then enhanced by glucocorticoid (data not shown). This suggests that a gene expression-dependent event in addition to the delayed loss of p38 MAPK activity is necessary for synergy.

Finally, TLR2 has variously been suggested to elicit both proinflammatory and anti-inflammatory effects (58, 59, 83), or even be a nonfunctional decoy (63). Given the high levels of TLR2 expression induced by IL1B-plus-glucocorticoid, we explored whether this newly expressed TLR2 was functionally active. In A549 and pHBECS that had been pretreated with IL1B-plus-dexamethasone, agonism of TLR2 significantly increased NF- κ B and IRF1-dependent reporter activity. This also led to the release of the proinflammatory mediators, CXCL8 and CCL5, which are here used as representative inflammatory responses. Thus, when induced by inflammatory cytokine combined with glucocorticoid, TLR2 behaves like other TLR- and IL-1 type receptors to promote inflammatory responses (84). Consistent with the ideas presented by Busillo *et al.* (56), we postulate that synergy at TLR2 may allow inflammatory responses to occur, for example, as a part of the innate immune response. As these effects may occur despite the local release of glucocorticoids that will more generally act to resolve inflammation, future studies will be needed to explore functional roles for TLR2 both in the absence and presence of glucocorticoids.

In conclusion, we show synergy between inflammatory cytokines and glucocorticoids to induce TLR2 expression in cell

Cytokine and glucocorticoid synergy on TLR2 expression

lines and in primary human airway epithelial cells. We identify novel enhancers upstream of human *TLR2* that bind GR and NF- κ B in cell lines and in pHBECS. These regions, along with GR and NF- κ B, appear to be important for synergy between glucocorticoids and the cytokines, IL1B and TNF. Unlike other inflammatory genes, TLR2 expression is transcriptionally enhanced following p38 α MAPK inhibition. As p38 MAPK is inhibited by glucocorticoids, we present a model whereby cooperativity between NF- κ B and GR, acting *via* R1 and R2 upstream of *TLR2*, combined with delayed glucocorticoid inhibition of p38 α , contribute to synergy (Fig. 10). TLR2 can then respond to activating ligands and promotes inflammatory responses. This may be a part of the normal host defense response, for example, by promoting pathogen clearance. However, such effects require careful examination in conditions such as severe asthma, COPD, or possibly viral infections, where anti-inflammatory effects of therapeutic glucocorticoid treatment could be compromised by inflammatory responses consequent on increased TLR2 expression. These considerations may be particularly important where TLR2 ligands are variously generated during infection, for example, SARS-CoV-2 (85), or as a result of infection-free inflammation (86). On one hand, increased TLR2 signaling could be beneficial in reducing the shedding of SARS-CoV-2 (87), whereas increasing inflammation in asthma or COPD is likely to be detrimental.

Experimental procedures

Drugs, inhibitors, and stimuli

Recombinant human IL1 β (R&D Systems) and TNF- α (R&D Systems) were dissolved in PBS containing 0.1% bovine serum albumin (Sigma-Aldrich). Budesonide (gift from AstraZeneca), dexamethasone (Sigma-Aldrich), SB203580 (Calbiochem), JNK-IN-VIII (Calbiochem), U0126 (Calbiochem), BIRB796 (Tocris), and VX745 (Tocris) were dissolved in dimethyl sulfoxide as stocks of 10 μ M. Toll-like receptor 2 agonists, Pam2CSK4, and Pam3CSK4 (both Invivogen) were prepared as stocks of 1 mg/ml in sterile water.

Submersion cell culture

The human pulmonary type II epithelial cell line, A549 (American Type Culture Collection CCL-185) was cultured in Dulbecco's modified Eagle's medium (DMEM) supplemented with 10% fetal bovine serum and 2 mM L-glutamine (all from Thermo Fisher Scientific). The human bronchial epithelial cell line, BEAS-2B (American Type Culture Collection CRL-9609), was grown in DMEM/F12 (Thermo Fisher Scientific) supplemented with 10% fetal bovine serum and 2 mM L-glutamine. Primary human bronchial epithelial cells were isolated from nontransplanted normal human lungs through the tissue retrieval service at the International Institute for the Advancement of Medicine, as previously described (88). No personal identifying information was provided for donors, and local ethics approval was granted by the Conjoint Health Research Ethics Board of the University of Calgary. The cells were grown in submersion culture in complete airway

epithelial cell medium (PromoCell). All cells were incubated at 37 °C in 5% CO₂:95% air and passaged when 90 to 95% confluent. Prior to all experiments, the cells were incubated overnight with serum- and additive-free basal medium to arrest cell growth.

Air-liquid interface culture of pHBECS

Primary human bronchial epithelial cells were grown in ALI culture as previously described (89, 90). Primary human bronchial epithelial cells were seeded in PneumaCult-EX expansion medium (05009, StemCell) containing 50X Supplement (05019, StemCell), 25 μ g/ml fluconazole (F8929, Sigma-Aldrich), 100 U/ml penicillin/streptomycin (15140-122, Thermo Fisher Scientific), and 1 μ M hydrocortisone (07904, StemCell). The cells were supplemented with fresh growth medium every 48 h until 90% confluent. Cells were then lifted using Trypsin/EGTA (CC-5012, Lonza) and Trypsin Neutralizing Solution (CC-5002, Lonza), seeded at 2.0×10^5 cells/cm² onto the apical surface of transwell inserts (3408, Corning) coated with bovine collagen Type I/III (5005-B, Advanced BioMatrix), and maintained at 37 °C, 5% CO₂. After 48 h, growth medium from the apical surface was removed to expose cells to air and the basal growth medium replaced with differentiation medium (PneumaCult-ALI basal medium (05002, StemCell) containing PneumaCult-ALI supplement (05003, StemCell), 25 μ g/ml fluconazole, 100 U/ml penicillin/streptomycin, 1 μ M hydrocortisone, and 4 μ g/ml heparin (07980, StemCell)). Cells were fed basally every 48 h with differentiation medium. From 14 days post seeding into transwell inserts, cells were washed apically once per week with PBS to remove excess mucus resulting from goblet cell differentiation. Five to six weeks post transwell seeding, highly differentiated ALI cultures were used for experiments. Air-liquid interface cultures were fed basally with PneumaCult-ALI basal medium, with no supplements, 18 h prior to experiments. The cells were then washed with PBS to remove excess mucus prior to apical and basolateral application of fresh medium containing drugs and stimuli. Apical treatments were diluted in 0.025 M Hepes in F12 (200 μ l/well), and basolateral treatments were diluted in PneumaCult-ALI basal medium (1 ml/well).

RNA extraction, cDNA synthesis, and qPCR

Total RNA was extracted using the NucleoSpin RNA Extraction kit (MN-740955, Macherey-Nagel), and 500 ng RNA was used for cDNA synthesis by qScript cDNA Synthesis Kit (CA101414-098, Quantabio). The resultant cDNA was diluted 1:5 with RNase-free water and stored at -20 °C. PCR was carried out using 2.5 μ l of cDNA using Fast SYBR Green Master Mix (4385618, Thermo Fisher Scientific) and primers specific for genes/regions of interest (Table S2). StepOnePlus (Applied Biosciences) or QuantStudio3 (Thermo Fisher Scientific) PCR systems were utilized for qPCR analysis. Relative cDNA concentrations were obtained from standard curves generated by half-log serial dilution of a stimulated cDNA sample and analyzed at the same time as

experimental samples. The quantity of the target from two technical replicates was averaged and normalized to the mean quantity of GAPDH determined from the same cDNA sample. The conditions for amplifications were as follows: 95 °C for 20 s, then 40 cycles of 95 °C for 3 s and 60 °C for 30 s. All primers were designed using NCBI PrimerBLAST and synthesized by the DNA synthesis lab at the University of Calgary or Thermo Fisher Scientific. Primer specificity was assessed through primer melt curve analysis using the following conditions: 95 °C for 3 s, 60 °C for 30 s followed by ramping to 95 °C at 0.1 °C/s with continuous fluorescent measurement. A single peak in the change of fluorescence with temperature was an indicative of acceptable primer specificity.

Analysis of unspliced nuclear TLR2 RNA

Nascent transcripts/unRNA accumulate transiently in the nucleus post transcriptional activation and can be used as a proxy of gene transcription (16, 78, 91). Toll-like receptor 2 unRNA was measured using SYBR Green primers spanning the intron2/exon3 junction of the *TLR2* gene. Primer sequences are shown in Table S2. Expression was normalized using abundant small nuclear RNA, U6. Each RNA sample was subjected to reverse transcription both in the presence and absence of reverse transcriptase to assess the signal due to genomic DNA contamination. The presence of an amplification product in the reverse transcriptase-negative samples was indicative of genomic DNA contamination. Samples with >15% genomic DNA contamination for either U6 or TLR2 were excluded from the analysis.

Western blotting

Western blotting was carried out as described previously (39). Following cell lysis, proteins were size-fractionated in SDS-PAGE gels. Following electrophoresis, the proteins were transferred to a nitrocellulose membrane followed by blocking and probing with primary antibodies against TLR2 (12276, Cell Signaling and ab108998, Abcam), GFP (2555, Cell Signaling), I κ B α (sc-371, SantaCruz), Ser32/Ser36 phosphorylated-I κ B α (9246, Cell Signaling), p65 (sc-8008, SantaCruz), Ser536 phosphorylated-p65 (3036, Cell Signaling), GR (PA1-511A, Thermo Fisher Scientific), MAPKAPK2 (3042, Cell Signaling), Thr334 phosphorylated-MAPKAPK2 (3041, Cell Signaling), total p38 (9212, Cell Signaling), Thr180/Tyr182 phosphorylated-p38 (9211, Cell Signaling), p38 α (9218, Cell Signaling), p38 β (2339, Cell Signaling), or GAPDH (MCA4739, Bio-Rad), overnight at 4 °C. Membranes were washed in Tris Buffer Saline-Tween 20 followed by incubation with 1:5000 or 1:10,000 dilution of the respective rabbit or mouse horseradish peroxidase-conjugated secondary immunoglobulin (Jackson ImmunoResearch) at room temperature. Membranes were washed 4 \times 5 min prior to detection of immune complexes by enhanced chemiluminescence (Bio-Rad). Images were acquired using a ChemiDoc Touch imaging system (Bio-Rad), and densitometric analysis was performed using ImageLab software (Bio-Rad).

Chromatin immunoprecipitation

Chromatin immunoprecipitation was performed in A549 or pHBECS as described previously (92). Briefly, A549 or pHBECS were grown to 90% confluency in 100 mm or 6-well culture plates, respectively. Proteins were cross-linked to DNA using 1% formaldehyde at room temperature for 10 min followed by quenching with 125 mM glycine for 5 min. Cells were then rinsed and washed twice with ice-cold HBSS, collected by scraping, and subjected to cytoplasmic and nuclei lysis in the presence of protease and phosphatase inhibitors at ice-cold temperature. Lysates were sonicated at 4 °C to shear DNA to an average fragment size of 200 to 500 bp and subjected to immunoprecipitation using magnetic beads incubated overnight with 10 μ g GR-356 (45) or p65 (8242, Cell Signaling) antibody. Post immunoprecipitation, the beads were washed with high- and low-salt buffers, and the cross-links were reversed in the presence of proteinase K. DNA was then purified using a ChIP DNA Clean & Concentrator kit (D5205, Zymo Research), and qPCR was performed using Fast SYBR Green Master Mix (Thermo Fisher Scientific) as described above. To analyze GR ChIP samples, ChIP-qPCR primers were designed flanking a GR binding site upstream to the *FKBP5* gene (used as positive control) as well as the two GR-binding regions upstream of *TLR2* gene, as identified in the GR ChIP-seq data in BEAS-2B and A549 cells. Chromatin immunoprecipitation-qPCR primers were also designed to amplify the RELA-binding region upstream to the *IL8* gene (used as a positive control) as well as the region showing RELA-binding upstream to the *TLR2* gene based on the p65 ChIP-seq data in BEAS-2B cells. Relative occupancy at each region was calculated as $\Delta\Delta C_T$ after normalization to the geometric mean of C_T values for three negative control regions, *OLIG3*, *MYOD1*, and *MYOG*, not predicted to be occupied by GR. Primer pairs are listed in Table S3.

Short interfering RNA-mediated knockdown

A549 cells were plated at approximately 70% confluency. Pools of four non-targeting siRNAs (SI03650325, SI03650318, SI04380467, 1022064), GR siRNA, MAPK14 (p38 α), MAPK11 (p38 β) siRNA, or TLR2 siRNA (all from Qiagen) were mixed with 3 μ l Lipofectamine RNAiMax (13778150, Thermo Fisher Scientific) in 100 μ l Opti-MEM (31985070, Thermo Fisher Scientific) and then incubated at room temperature for 5 min. This mixture was then added to the cells in serum-containing growth medium and incubated for 24 to 48 h until cells were >90% confluent.

Luciferase reporter constructs and assay

A549 cells containing the NF- κ B reporter, 6 κ Btk.luc, and the GRE reporter, 2 \times GRE.luc have been generated as previously described (44, 93). A *KpnI-XbaI* fragment from a 6 \times IRF1 luciferase reporter (Panomics) containing the IRF1 sites and luciferase gene was used to replace the equivalent region in pGL3.basic.neo prior to stable transfection into A549 cells as described (44, 93). To generate R1/R2-luc constructs, primers were designed to amplify regions R1 and R2

Cytokine and glucocorticoid synergy on TLR2 expression

(557 bp and 658 bp, respectively) from upstream of the *TLR2* locus (Table S4) using Platinum SuperFi PCR Master Mix (12358010, Thermo Fisher Scientific). Polymerase chain reaction products were then introduced into linearized and topoisomerase I-activated PCR Blunt II-TOPO vector (450245, Thermo Fisher Scientific), followed by subcloning into the empty pGL3.TATA.neo vector (38) using *KpnI* (R3142, New England Biolabs) and *XhoI* (R0146, New England Biolabs) enzymes. To generate R1+R2-luc constructs, R1 was reamplified from R1-luc using primers containing flanking restriction sites for *KpnI* and *SacI*. Similarly, primers containing restriction sites for *SacI* and *XhoI* were designed to reamplify R2 from R2-luc. These PCR products were then purified and religated into *KpnI/XhoI*-digested empty pGL3.TATA.neo vector. Deletion of the GRE and RELA sites was performed using the Q5 Site-Directed Mutagenesis Kit as per manufacturer's protocol (E0554S, New England Biolabs). Primers for site-directed mutagenesis were designed using the online tool NEBaseChanger (<https://nebasechanger.neb.com/>). Primers used for cloning and mutagenesis are listed in Table S4. Each plasmid (12 µg) and the empty vector (as control) were transfected into preconfluent A549 cells in T-75 flasks using Lipofectamine 2000 (11668019, Thermo Fisher Scientific) 24 h prior to the addition of 1 mg/ml G418 (Sigma-Aldrich). After 14 to 21 days, foci of G418-resistant cells were passaged in the presence of G418 (0.6 mg/ml) prior to cryo-storage for future experiments. Reporter assays were performed using the Firefly Luciferase Assay Kit 2.0 (30085, Biotium Inc) according to manufacturer's protocol.

Adenovirus infection

As previously described (41), cells at ~70% confluency were infected with indicated MOI of either IκBαΔN or GFP-expressing adenoviral vector (Ad5-IκBαΔN or Ad5-GFP, respectively) in serum-containing medium. After 24 h, the cells were incubated overnight in serum- and additive-free basal medium prior to treatments.

Enzyme-linked immunosorbent assay

Supernatants were collected from the cells after experiments and frozen prior to measuring cytokine release. CXCL8 was quantified using sandwich ELISA as previously described (94). CCL5 was measured using a human CCL5 DuoSet ELISA kit from R&D Systems.

Data presentation and statistical analysis

GraphPad Prism 5 software was used for generating data figures and performing statistical analysis. Data are plotted as box-and-whiskers plots, where boxes represent lower and upper quartile median values and whiskers indicate min-max values, or as bar or line graphs showing means ± S.E. For normally distributed data, multiple comparison between groups were made by one-way ANOVA, with the appropriate post-hoc test (Sidak's or Dunnett's), as indicated. Equivalent nonparametric tests were utilized for non-normal distribution.

Two-tailed, paired Student's *t* test was used for comparing two treatment groups. 'N' in the graphs represents the number of independent experiments. To test for greater than simple additivity, the sum of the effects (*i.e.*, fold - 1) of each treatment (IL1B, TNF, or glucocorticoid alone) (*sum*) was compared to the effect of cotreatment (*comb*). Chromatin immunoprecipitation-seq and GRO-seq data were visualized using UCSC Genome Browser (<https://genome.ucsc.edu/>). Glucocorticoid response element and RELA motifs upstream to the TLR2 promoter regions were identified using JASPAR CORE 2020 track in UCSC Genome Browser (47).

Data availability

All the data produced for this work are contained within the article and the supporting information.

Supporting information—This article contains supporting information. (46, 47)

Acknowledgments—The authors would like to thank Dr David Proud for assistance with the provision of pHBECS and for supervision of Aubrey Michi. We also would like to acknowledge the Canadian Fund of Innovation (CFI) and the Alberta Science and Research Authority for providing an equipment and infrastructure grant to perform real-time PCR.

Author contributions—A. B. and R. N. conceptualization; A. B. and R. N. methodology; C. K., R. L., and A. N. G. resources; A. B., M. M. M., C. K., S. K. S., A. N. M., and S. V. S. investigation; A. B. formal analysis; A. B. and R. N. writing—original draft; A. B., M. M. M., C. K., S. K. S., A. N. M., S. V. S., R. L., A. N. G., and R. N. writing—review and editing.

Funding and additional information—This work was supported by the following: R. N. grants: Canadian Institutes of Health Research (CIHR) (MOP 125918, PJT 156310) and Natural Sciences and Engineering Research Council of Canada (NSERC) discovery grant (RGPIN- 2016-04549); A. B. studentships: Eyes High Doctoral Scholarship and Eleanor Mackie Doctoral Scholarship in Women's Health from University of Calgary; M. M. M. studentships: NSERC Postgraduate Scholarship - Doctoral, Queen Elizabeth II Doctoral scholarship, and The Lung Association—Alberta & NWT student-ship awards. The funding bodies played no role in the design of the study and collection, analysis, and interpretation of data.

Conflict of interest—The authors declare that they have no conflicts of interest with the contents of this article.

Abbreviations—The abbreviations used are: Ad5, adenovirus serotype 5; ALI, air-liquid interface; ChIP, chromatin immunoprecipitation; COPD, chronic obstructive pulmonary disease; DUSP1, dual-specificity phosphatase 1; eRNA, enhancer RNA; GR, glucocorticoid receptor; GRE, glucocorticoid response element; GRO-seq, global run-on followed by sequencing; IL1B, interleukin-1β; IRF1, interferon regulatory factor 1; JNK-IN-VIII, JNK inhibitor VIII; MAPK, mitogen-activated protein kinase; MK2, MAPK-activated protein kinase 2; MOI, multiplicity of infection; NF-κB, nuclear factor-κB; pHBECS, primary human bronchial epithelial cells;

qPCR, quantitative PCR; TLR, toll-like receptor; TNF, tumor necrosis factor α ; unRNA, unspliced nuclear RNA.

References

- Rhen, T., and Cidlowski, J. A. (2005) Antiinflammatory action of glucocorticoids — new mechanisms for old drugs. *N. Engl. J. Med.* **353**, 1711–1723
- Barnes, P. J. (2006) Corticosteroids: The drugs to beat. *Eur. J. Pharmacol.* **533**, 2–14
- Barnes, P. J. (2013) Corticosteroid resistance in patients with asthma and chronic obstructive pulmonary disease. *J. Allergy Clin. Immunol.* **131**, 636–645
- Liu, D., Ahmet, A., Ward, L., Krishnamoorthy, P., Mandelcorn, E. D., Leigh, R., Brown, J. P., Cohen, A., and Kim, H. (2013) A practical guide to the monitoring and management of the complications of systemic corticosteroid therapy. *Allergy Asthma Clin. Immunol.* **9**, 30
- Lambrecht, B. N., and Hammad, H. (2012) The airway epithelium in asthma. *Nat. Med.* **18**, 684–692
- Diamond, G., Legarda, D., and Ryan, L. K. (2000) The innate immune response of the respiratory epithelium. *Immunol. Rev.* **173**, 27–38
- Gras, D., Chanez, P., Vachier, I., Petit, A., and Bourdin, A. (2013) Bronchial epithelium as a target for innovative treatments in asthma. *Pharmacol. Ther.* **140**, 290–305
- Klaßen, C., Karabinskaya, A., Dejager, L., Vettorazzi, S., Van Moorleghem, J., Lühder, F., Meijnsing, S. H., Tuckermann, J. P., Bohnenberger, H., Libert, C., and Reichardt, H. M. (2017) Airway epithelial cells are crucial targets of glucocorticoids in a mouse model of allergic asthma. *J. Immunol.* **199**, 48–61
- Barnes, P. J. (2010) Mechanisms and resistance in glucocorticoid control of inflammation. *J. Steroid Biochem. Mol. Biol.* **120**, 76–85
- Jantzen, H. M., Strähle, U., Gloss, B., Stewart, F., Schmid, W., Boshart, M., Miksicek, R., and Schütz, G. (1987) Cooperativity of glucocorticoid response elements located far upstream of the tyrosine aminotransferase gene. *Cell* **49**, 29–38
- Imai, E., Stromstedt, P. E., Quinn, P. G., Carlstedt-Duke, J., Gustafsson, J. A., and Granner, D. K. (1990) Characterization of a complex glucocorticoid response unit in the phosphoenolpyruvate carboxykinase gene. *Mol. Cell. Biol.* **10**, 4712–4719
- De Bosscher, K., and Haegeman, G. (2009) Minireview: Latest perspectives on antiinflammatory actions of glucocorticoids. *Mol. Endocrinol.* **23**, 281–291
- Scheinman, R. I., Cogswell, P. C., Lofquist, A. K., and Baldwin, A. S. (1995) Role of transcriptional activation of I κ B α in mediation of immunosuppression by glucocorticoids. *Science* **270**, 283–286
- Altonsy, M. O., Sasse, S. K., Phang, T. L., and Gerber, A. N. (2014) Context-dependent cooperation between nuclear factor κ B (NF- κ B) and the glucocorticoid receptor at a TNFAIP3 intronic enhancer: A mechanism to maintain negative feedback control of inflammation. *J. Biol. Chem.* **289**, 8231–8239
- Smoak, K., and Cidlowski, J. A. (2006) Glucocorticoids regulate tristetraprolin synthesis and posttranscriptionally regulate tumor necrosis factor Alpha inflammatory signaling. *Mol. Cell. Biol.* **26**, 9126–9135
- King, E. M., Kaur, M., Gong, W., Rider, C. F., Holden, N. S., and Newton, R. (2009) Regulation of tristetraprolin expression by interleukin-1 β and dexamethasone in human pulmonary epithelial cells: Roles for nuclear factor- κ B and p38 mitogen-activated protein kinase. *J. Pharmacol. Exp. Ther.* **330**, 575–585
- Leigh, R., Mostafa, M. M., King, E. M., Rider, C. F., Shah, S., Dumonceaux, C., Traves, S. L., McWhae, A., Kolisnik, T., Kooi, C., Slater, D. M., Kelly, M. M., Bieda, M., Miller-Larsson, A., and Newton, R. (2016) An inhaled dose of budesonide induces genes involved in transcription and signaling in the human airways: Enhancement of anti- and proinflammatory effector genes. *Pharmacol. Res. Perspect.* **4**, e00243
- Kelly, M. M., King, E. M., Rider, C. F., Gwozd, C., Holden, N. S., Eddleston, J., Zuraw, B., Leigh, R., O'Byrne, P. M., and Newton, R. (2012) Corticosteroid-induced gene expression in allergen-challenged asthmatic subjects taking inhaled budesonide. *Br. J. Pharmacol.* **165**, 1737–1747
- Ayrolidi, E., and Riccardi, C. (2009) Glucocorticoid-induced leucine zipper (GILZ): A new important mediator of glucocorticoid action. *FASEB J.* **23**, 3649–3658
- Mostafa, M. M., Rider, C. F., Shah, S., Traves, S. L., Gordon, P. M. K., Miller-Larsson, A., Leigh, R., and Newton, R. (2019) Glucocorticoid-driven transcriptomes in human airway epithelial cells: Commonalities, differences and functional insight from cell lines and primary cells. *BMC Med. Genomics* **12**, 1–21
- Kassel, O., Sancono, A., Krätzschmar, J., Kreft, B., Stassen, M., and Cato, A. C. B. (2001) Glucocorticoids inhibit MAP kinase *via* increased expression and decreased degradation of MKP-1. *EMBO J.* **20**, 7108–7116
- Oh, K. S., Patel, H., Gottschalk, R. A., Lee, W. S., Baek, S., Fraser, I. D. C., Hager, G. L., and Sung, M. H. (2017) Anti-inflammatory chromatin landscape suggests alternative mechanisms of glucocorticoid receptor action. *Immunity* **47**, 298–309.e5
- Newton, R., Shah, S., Altonsy, M. O., and Gerber, A. N. (2017) Glucocorticoid and cytokine crosstalk: Feedback, feedforward, and co-regulatory interactions determine repression or resistance. *J. Biol. Chem.* **292**, 7163–7172
- Hofmann, T. G., and Lienhard, M. (2002) The promoter context determines mutual repression or synergism between NF- κ B and the glucocorticoid receptor. *Biol. Chem.* **383**, 1947–1951
- Rao, N. A. S., McCalman, M. T., Moulos, P., Francoijs, K. J., Chatziioannou, A., Kolisis, F. N., Alexis, M. N., Mitsiou, D. J., and Stunnenberg, H. G. (2011) Coactivation of GR and NF κ B alters the repertoire of their binding sites and target genes. *Genome Res.* **21**, 1404–1416
- Kadiyala, V., Sasse, S. K., Altonsy, M. O., Berman, R., Chu, H. W., Phang, T. L., and Gerber, A. N. (2016) Cistrome-based cooperation between airway epithelial glucocorticoid receptor and NF- κ B orchestrates anti-inflammatory effects. *J. Biol. Chem.* **291**, 12673–12687
- Miyata, M., Lee, J.-Y., Susuki-Miyata, S., Wang, W. Y., Xu, H., Kai, H., Kobayashi, K. S., Flavell, R. A., and Li, J.-D. (2015) Glucocorticoids suppress inflammation *via* the upregulation of negative regulator IRAK-M. *Nat. Commun.* **6**, 6062
- Shah, S., King, E. M., Mostafa, M. M., Altonsy, M. O., and Newton, R. (2016) DUSP1 maintains IRF1 and leads to increased expression of IRF1-dependent genes: A mechanism promoting glucocorticoid insensitivity. *J. Biol. Chem.* **291**, 21802–21816
- Hermoso, M. A., Matsuguchi, T., Smoak, K., and Cidlowski, J. A. (2004) Glucocorticoids and tumor necrosis factor alpha cooperatively regulate toll-like receptor 2 gene expression. *Mol. Cell. Biol.* **24**, 4743–4756
- Shuto, T., Imasato, A., Jono, H., Sakai, A., Xu, H., Watanabe, T., Rixter, D. D., Kai, H., Andalibi, A., Linthicum, F., Guan, Y. L., Han, J., Cato, A. C. B., Lim, D. J., Akira, S., *et al.* (2002) Glucocorticoids synergistically enhance nontypeable Haemophilus influenzae-induced toll-like receptor 2 expression *via* a negative cross-talk with p38 MAP kinase. *J. Biol. Chem.* **277**, 17263–17270
- Sakai, A., Han, J., Cato, A. C. B., Akira, S., and Li, J. D. (2004) Glucocorticoids synergize with IL-1 β to induced TLR2 expression *via* MAP kinase phosphatase-1-dependent dual inhibition of MAPK JNK and p38 in epithelial cells. *BMC Mol. Biol.* **5**, 2
- Akira, S., Takeda, K., and Kaisho, T. (2001) Toll-like receptors: Critical proteins linking innate and acquired immunity. *Nat. Immunol.* **2**, 675–680
- Yoshimura, A., Lien, E., Ingalls, R. R., Tuomanen, E., Dziarski, R., and Golenbock, D. (1999) Cutting edge: Recognition of gram-positive bacterial cell wall components by the innate immune system occurs *via* toll-like receptor 2. *J. Immunol.* **163**, 1–5
- Schwandner, R., Dziarski, R., Wesche, H., Rothe, M., and Kirschning, C. J. (1999) Peptidoglycan- and lipoteichoic acid-induced cell activation is mediated by toll-like receptor 2. *J. Biol. Chem.* **274**, 17406–17409
- Brightbill, H. D., Libraty, D. H., Krutzik, S. R., Yang, R. B., Belisle, J. T., Bleharski, J. R., Maitland, M., Norgard, M. V., Plevy, S. E., Smale, S. T., Brennan, P. J., Bloom, B. R., Godowski, P. J., and Modlin, R. L. (1999) Host defense mechanisms triggered by microbial lipoproteins through toll-like receptors. *Science* **285**, 732–736

Cytokine and glucocorticoid synergy on TLR2 expression

36. Newton, R., Adcock, I. M., and Barnes, P. J. (1996) Superinduction of NF- κ B by actinomycin D and cycloheximide in epithelial cells. *Biochem. Biophys. Res. Commun.* **218**, 518–523
37. Newton, R., Holden, N. S., Catley, M. C., Oyelusi, W., Leigh, R., Proud, D., and Barnes, P. J. (2007) Repression of inflammatory gene expression in human pulmonary epithelial cells by small-molecule I B kinase inhibitors. *J. Pharmacol. Exp. Ther.* **321**, 734–742
38. Catley, M. C., Cambridge, L. M., Nasuhara, Y., Ito, K., Chivers, J. E., Beaton, A., Holden, N. S., Bergmann, M. W., Barnes, P. J., and Newton, R. (2004) Inhibitors of protein kinase C (PKC) prevent activated transcription: Role of events downstream of NF- κ B DNA binding. *J. Biol. Chem.* **279**, 18457–18466
39. King, E. M., Holden, N. S., Gong, W., Rider, C. F., and Newton, R. (2009) Inhibition of NF- κ -dependent transcription by MKP-1. Transcriptional repression by glucocorticoids occurring via p38 MAPK. *J. Biol. Chem.* **284**, 26803–26815
40. Rider, C. F., Shah, S., Miller-Larsson, A., Giembycz, M. A., and Newton, R. (2015) Cytokine-induced loss of glucocorticoid function: Effect of kinase inhibitors, long-acting β 2-adrenoceptor agonist and glucocorticoid receptor ligands. *PLoS One* **10**, e0116773
41. Catley, M. C., Chivers, J. E., Holden, N. S., Barnes, P. J., and Newton, R. (2005) Validation of IKK beta as therapeutic target in airway inflammatory disease by adenoviral-mediated delivery of dominant-negative IKK beta to pulmonary epithelial cells. *Br. J. Pharmacol.* **145**, 114–122
42. Castro, A. C., Dang, L. C., Soucy, F., Grenier, L., Mazdiyasi, H., Hottelet, M., Parent, L., Pien, C., Palombella, V., and Adams, J. (2003) Novel IKK inhibitors: β -Carbolines. *Bioorg. Med. Chem. Lett.* **13**, 2419–2422
43. Hideshima, T., Chauhan, D., Richardson, P., Mitsiades, C., Mitsiades, N., Hayashi, T., Munshi, N., Dang, L., Castro, A., Palombella, V., Adams, J., and Anderson, K. C. (2002) NF- κ B as a therapeutic target in multiple myeloma. *J. Biol. Chem.* **277**, 16639–16647
44. Chivers, J. E., Cambridge, L. M., Catley, M. C., Mak, J. C., Donnelly, L. E., Barnes, P. J., and Newton, R. (2004) Differential effects of RU486 reveal distinct mechanisms for glucocorticoid repression of prostaglandin E2 release. *Eur. J. Biochem.* **271**, 4042–4052
45. Sasse, S. K., Gruca, M., Allen, M. A., Kadiyala, V., Song, T., Gally, F., Gupta, A., Pufall, M. A., Dowell, R. D., and Gerber, A. N. (2019) Nascent transcript analysis of glucocorticoid crosstalk with TNF defines primary and cooperative inflammatory repression. *Genome Res.* **29**, 1753–1765
46. Dunham, I., Kundaje, A., Aldred, S. F., Collins, P. J., Davis, C. A., Doyle, F., Epstein, C. B., Frietze, S., Harrow, J., Kaul, R., Khatun, J., Lajoie, B. R., Landt, S. G., Lee, B. K., Pauli, F., et al. (2012) An integrated encyclopedia of DNA elements in the human genome. *Nature* **489**, 57–74
47. Fornes, O., Castro-Mondragon, J. A., Khan, A., Van Der Lee, R., Zhang, X., Richmond, P. A., Modi, B. P., Correard, S., Gheorghe, M., Baranašić, D., Santana-Garcia, W., Tan, G., Chèneby, J., Ballester, B., Parcy, F., et al. (2020) JASPAR 2020: Update of the open-access database of transcription factor binding profiles. *Nucleic Acids Res.* **48**, D87–D92
48. Ambrosini, G., Groux, R., and Bucher, P. (2018) PWMScan: A fast tool for scanning entire genomes with a position-specific weight matrix. *Bioinformatics* **34**, 2483–2484
49. Shah, S., King, E. M., Chandrasekhar, A., and Newton, R. (2014) Roles for the mitogen-activated protein kinase (MAPK) phosphatase, DUSP1, in feedback control of inflammatory gene expression and repression by dexamethasone. *J. Biol. Chem.* **289**, 13667–13679
50. Davis, M. I., Hunt, J. P., Herrgard, S., Ciceri, P., Wodicka, L. M., Pallares, G., Hocker, M., Treiber, D. K., and Zarrinkar, P. P. (2011) Comprehensive analysis of kinase inhibitor selectivity. *Nat. Biotechnol.* **29**, 1046–1051
51. Freshney, N. W., Rawlinson, L., Guesdon, F., Jones, E., Cowley, S., Hsuan, J., and Saklatvala, J. (1994) Interleukin-1 activates a novel protein kinase cascade that results in the phosphorylation of hsp27. *Cell* **78**, 1039–1049
52. Jin, M. S., Kim, S. E., Heo, J. Y., Lee, M. E., Kim, H. M., Paik, S. G., Lee, H., and Lee, J. O. (2007) Crystal structure of the TLR1-TLR2 heterodimer induced by binding of a tri-acylated lipopeptide. *Cell* **130**, 1071–1082
53. Kang, J. Y., Nan, X., Jin, M. S., Youn, S. J., Ryu, Y. H., Mah, S., Han, S. H., Lee, H., Paik, S. G., and Lee, J. O. (2009) Recognition of lipopeptide patterns by toll-like receptor 2-Toll-like receptor 6 heterodimer. *Immunity* **31**, 873–884
54. Schleimer, R. P. (2004) Glucocorticoids suppress inflammation but spare innate immune responses in airway epithelium. *Proc. Am. Thorac. Soc.* **1**, 222–230
55. Cruz-Topete, D., and Cidlowski, J. A. (2014) One hormone, two actions: Anti- and pro-inflammatory effects of glucocorticoids. *Neuro-immunomodulation* **22**, 20–32
56. Busillo, J. M., and Cidlowski, J. A. (2013) The five Rs of glucocorticoid action during inflammation: Ready, reinforce, repress, resolve, and restore. *Trends Endocrinol. Metab.* **24**, 109–119
57. Busillo, J. M., Azzams, K. M., and Cidlowski, J. A. (2011) Glucocorticoids sensitize the innate immune system through regulation of the NLRP3 inflammasome. *J. Biol. Chem.* **286**, 38703–38713
58. Imasato, A., Desbois-Mouthon, C., Han, J., Kai, H., Cato, A. C. B., Akira, S., and Li, J. D. (2002) Inhibition of p38 MAPK by glucocorticoids via induction of MAPK phosphatase-1 enhances nontypeable haemophilus influenzae-induced expression of toll-like receptor 2. *J. Biol. Chem.* **277**, 47444–47450
59. Homma, T., Kato, A., Hashimoto, N., Batchelor, J., Yoshikawa, M., Imai, S., Wakiguchi, H., Saito, H., and Matsumoto, K. (2004) Corticosteroid and cytokines synergistically enhance toll-like receptor 2 expression in respiratory epithelial cells. *Am. J. Respir. Cell Mol. Biol.* **31**, 463–469
60. Kis, K., Bodai, L., Polyanka, H., Eder, K., Pivarcsi, A., Duda, E., Soos, G., Bata-Csorgo, Z., and Kemeny, L. (2006) Budesonide, but not tacrolimus, affects the immune functions of normal human keratinocytes. *Int. Immunopharmacol.* **6**, 358–368
61. Shibata, M., Katsuyama, M., Onodera, T., Ehama, R., Hosoi, J., and Tagami, H. (2009) Glucocorticoids enhance toll-like receptor 2 expression in human keratinocytes stimulated with propionibacterium acnes or proinflammatory cytokines. *J. Invest. Dermatol.* **129**, 375–382
62. Su, Q., Pfalzgraff, A., and Weindl, G. (2017) Cell type-specific regulatory effects of glucocorticoids on cutaneous TLR2 expression and signalling. *J. Steroid Biochem. Mol. Biol.* **171**, 201–208
63. Hoppstädter, J., Dembek, A., Linnenberger, R., Dahlem, C., Barghash, A., Fecher-Trost, C., Fuhrmann, G., Koch, M., Kraegeloh, A., Huwer, H., and Kierner, A. K. (2019) Toll-like receptor 2 release by macrophages: An anti-inflammatory program induced by glucocorticoids and lipopolysaccharide. *Front. Immunol.* **10**, 1634
64. McDowell, I. C., Barrera, A., D’Ippolito, A. M., Vockley, C. M., Hong, L. K., Leichter, S. M., Bartelt, L. C., Majoros, W. H., Song, L., Safi, A., Koçak, D. D., Gersbach, C. A., Hartemink, A. J., Crawford, G. E., Engelhardt, B. E., et al. (2018) Glucocorticoid receptor recruits to enhancers and drives activation by motif-directed binding. *Genome Res.* **28**, 1272–1284
65. Heinz, S., Romanoski, C. E., Benner, C., and Glass, C. K. (2015) The selection and function of cell type-specific enhancers. *Nat. Rev. Mol. Cell Biol.* **16**, 144–154
66. Kim, T. K., and Shiekhattar, R. (2015) Architectural and functional commonalities between enhancers and promoters. *Cell* **162**, 948–959
67. Calo, E., and Wysocka, J. (2013) Modification of enhancer chromatin: What, how, and why? *Mol. Cell* **49**, 825–837
68. Zhu, Y., Sun, L., Chen, Z., Whitaker, J. W., Wang, T., and Wang, W. (2013) Predicting enhancer transcription and activity from chromatin modifications. *Nucleic Acids Res.* **41**, 10032–10043
69. Mousavi, K., Zare, H., Dell’Orso, S., Grontved, L., Gutierrez-Cruz, G., Derfoul, A., Hager, G. L., and Sartorelli, V. (2013) ERNAs promote transcription by establishing chromatin accessibility at defined genomic loci. *Mol. Cell* **51**, 606–617
70. Maruyama, A., Mimura, J., and Itoh, K. (2014) Non-coding RNA derived from the region adjacent to the human HO-1 E2 enhancer selectively regulates HO-1 gene induction by modulating Pol II binding. *Nucleic Acids Res.* **42**, 13599–13614
71. Li, W., Notani, D., Ma, Q., Tanasa, B., Nunez, E., Chen, A. Y., Merkurjev, D., Zhang, J., Ohgi, K., Song, X., Oh, S., Kim, H. S., Glass, C. K., and Rosenfeld, M. G. (2013) Functional roles of enhancer RNAs for oestrogen-dependent transcriptional activation. *Nature* **498**, 516–520
72. Hsieh, C. L., Fei, T., Chen, Y., Li, T., Gao, Y., Wang, X., Sun, T., Sweeney, C. J., Lee, G. S. M., Chen, S., Balk, S. P., Liu, X. S., Brown, M., and Kantoff, P. W. (2014) Enhancer RNAs participate in androgen receptor-

- driven looping that selectively enhances gene activation. *Proc. Natl. Acad. Sci. U. S. A.* **111**, 7319–7324
73. D'Ippolito, A. M., McDowell, I. C., Barrera, A., Hong, L. K., Leichter, S. M., Bartelt, L. C., Vockley, C. M., Majoros, W. H., Safi, A., Song, L., Gersbach, C. A., Crawford, G. E., and Reddy, T. E. (2018) Pre-established chromatin interactions mediate the genomic response to glucocorticoids. *Cell Syst.* **7**, 146–160.e7
 74. Vockley, C. M., D'Ippolito, A. M., McDowell, I. C., Majoros, W. H., Safi, A., Song, L., Crawford, G. E., and Reddy, T. E. (2016) Direct GR binding sites potentiate clusters of TF binding across the human genome. *Cell* **166**, 1269–1281.e19
 75. Ray, A., and Prefontaine, K. E. (1994) Physical association and functional antagonism between the p65 subunit of transcription factor NF- κ B and the glucocorticoid receptor. *Proc. Natl. Acad. Sci. U. S. A.* **91**, 752–756
 76. Zaret, K. S., and Carroll, J. S. (2011) Pioneer transcription factors: Establishing competence for gene expression. *Genes Dev.* **25**, 2227–2241
 77. Newton, R., and Holden, N. S. (2006) New aspects of p38 mitogen activated protein kinase (MAPK) biology in lung inflammation. *Drug Discov. Today Dis. Mech.* **3**, 53–61
 78. Newton, R., King, E. M., Gong, W., Rider, C. F., Staples, K. J., Holden, N. S., and Bergmann, M. W. (2010) Glucocorticoids inhibit IL-1 β -induced GM-CSF expression at multiple levels: Roles for the ERK pathway and repression by MKP-1. *Biochem. J.* **427**, 113–124
 79. Mylona, A., Theillet, F. X., Foster, C., Cheng, T. M., Miralles, F., Bates, P. A., Selenko, P., and Treisman, R. (2016) Opposing effects of Elk-1 multisite phosphorylation shape its response to ERK activation. *Science* **354**, 233–237
 80. Laine, A., and Ronai, Z. (2005) Ubiquitin chains in the ladder of MAPK signaling. *Sci. STKE* **2005**, re5
 81. Liu, S. Y., Ma, Y. L., Hsu, W. L., Chiou, H. Y., and Lee, E. H. Y. (2019) Protein inhibitor of activated STAT1 Ser503 phosphorylation-mediated Elk-1 SUMOylation promotes neuronal survival in APP/PS1 mice. *Br. J. Pharmacol.* **176**, 1793–1810
 82. Kukushkin, A. N., Abramova, M. V., Svetlikova, S. B., Darieva, Z. A., Pospelova, T. V., and Pospelov, V. A. (2002) Downregulation of c-fos gene transcription in cells transformed by E1A and cHa-ras oncogenes: A role of sustained activation of MAP/ERK kinase cascade and of inactive chromatin structure at c-fos promoter. *Oncogene* **21**, 719–730
 83. Winder, A. A., Wohlford-Lenane, C., Scheetz, T. E., Nardy, B. N., Manzel, L. J., Look, D. C., and McCray, P. B. (2009) Differential effects of cytokines and corticosteroids on toll-like receptor 2 expression and activity in human airway epithelia. *Respir. Res.* **10**, 96
 84. O'Neill, L. A. J., and Bowie, A. G. (2007) The family of five: TIR-domain-containing adaptors in toll-like receptor signalling. *Nat. Rev. Immunol.* **7**, 353–364
 85. Zheng, M., Karki, R., Williams, E. P., Yang, D., Fitzpatrick, E., Vogel, P., Jonsson, C. B., and Kanneganti, T. D. (2021) TLR2 senses the SARS-CoV-2 envelope protein to produce inflammatory cytokines. *Nat. Immunol.* **22**, 829–838
 86. Lorne, E., Dupont, H., and Abraham, E. (2010) Toll-like receptors 2 and 4: Initiators of non-septic inflammation in critical care medicine? *Intensive Care Med.* **36**, 1826–1835
 87. Proud, P. C., Tsitoura, D., Watson, R. J., Chua, B. Y., Aram, M. J., Bewley, K. R., Cavell, B. E., Cobb, R., Dowall, S., Fotheringham, S. A., Ho, C. M. K., Lucas, V., Ngabo, D., Rayner, E., Ryan, K. A., *et al.* (2021) Prophylactic intranasal administration of a TLR2/6 agonist reduces upper respiratory tract viral shedding in a SARS-CoV-2 challenge ferret model. *EBioMedicine* **63**, 103153
 88. Hudy, M. H., Traves, S. L., Wiehler, S., and Proud, D. (2010) Cigarette smoke modulates rhinovirus-induced airway epithelial cell chemokine production. *Eur. Respir. J.* **35**, 1256–1263
 89. Warner, S. M., Wiehler, S., Michi, A. N., and Proud, D. (2019) Rhinovirus replication and innate immunity in highly differentiated human airway epithelial cells. *Respir. Res.* **20**, 1–13
 90. Michi, A. N., and Proud, D. (2021) A toolbox for studying respiratory viral infections using air-liquid interface cultures of human airway epithelial cells. *Am. J. Physiol. Lung Cell Mol. Physiol.* **321**, 263–279
 91. Lipson, K. E., and Baserga, R. (1989) Transcriptional activity of the human thymidine kinase gene determined by a method using the polymerase chain reaction and an intron-specific probe. *Proc. Natl. Acad. Sci. U. S. A.* **86**, 9774–9777
 92. Mostafa, M. M., Bansal, A., Michi, A. N., Sasse, S. K., Proud, D., Gerber, A. N., and Newton, R. (2021) Genomic determinants implicated in the glucocorticoid-mediated induction of KLF9 in pulmonary epithelial cells. *J. Biol. Chem.* **296**, 100065
 93. Newton, R., Hart, L. A., Stevens, D. A., Bergmann, M., Donnelly, L. E., Adcock, I. M., and Barnes, P. J. (1998) Effect of dexamethasone on interleukin-1 β -(IL-1 β)-induced nuclear factor- κ B (NF- κ B) and κ B-dependent transcription in epithelial cells. *Eur. J. Biochem.* **254**, 81–89
 94. Subauste, M. C., Jacoby, D. B., Richards, S. M., and Proud, D. (1995) Infection of a human respiratory epithelial cell line with rhinovirus. Induction of cytokine release and modulation of susceptibility to infection by cytokine exposure. *J. Clin. Invest.* **96**, 549–557